gene expression and that both SCD-1 and SCD-2 play a role in the mechanism of fatty liver. As shown in results from our and other laboratories, chronic ethanol feeding increased levels of SCD-2, and SREBP-1c expression. Consistent with our results, Crabb et al.[33] recently reported that chronic ethanol feeding activates hepatic SREBP-1. Such suppressive actions of pioglitazone on up-regulation of these genes could greatly improve ethanol-induced hepatic steatosis cooperatively with its aforementioned effects on the lipid mobilization via VLDL as a whole.

Recently, HGF was reported to prevent LPS-induced hepatic sinusoidal endothelial cell injury and intrasinusoidal fibrin deposition in rats.[34] It has also been reported that the mere presence of fat in the liver leads to hepatic lipid peroxidation and that chronic steatosis is associated with persistent lipid peroxidation.[35] Lipid peroxidation is proposed as a mechanism of alcohol-induced hepatotoxicity. It has been suggested that chronic lipid peroxidation could represent the missing link between chronic steatosis and steatohepatitis. In our study, pioglitazone improved ethanol-induced lipid peroxidation and resultant cellular damages by increasing the c-Met expression and by decreasing hepatic fat amounts, as indicated by results showing suppression of antioxidative genes such as MT-1, -2, and HOX-1.[36,37] Furthermore, so far as judged from the current TUNEL analyses, pioglitazone treatment did not induce any notable apoptosis in liver. Such a cytoprotective feature of pioglitazone on ethanol-induced hepatic steatosis is likely to be of great clinical advantage in that other thiazolidinedione derivatives such as troglitazone have been reported to induce apoptotic hepatocyte death, leading to a conflict for its clinical use.[38] Based on these findings, we propose an important new mechanism to explain the recovery from alcoholic fatty liver in response to pioglitazone (i.e., that pioglitazone enhances c-Met expression in hepatocytes, resulting in activation of HGF/c-Met signaling). The HGF/c-Met signaling activation induced by pioglitazone leads to increased apoB synthesis with subsequent lipid mobilization of VLDL from hepatocytes, and decreases hepatic SCD levels with decreased synthesis of triglycerides in liver. Such an effect of pioglitazone could also stimulate regeneration and attenuate lipid peroxidation.

The current study suggesting usefulness of pioglitazone to treat ethanol-induced hepatic steatosis led us to hypothesize that such an HGF-mimicking hepatoprotective PPARγ ligand could clinically be used to limit fatty infiltration of the liver caused by other disease conditions. For instance, posttransplant fatty infiltration in the donor liver accounts for a serious complication causing primary nonfunction.[39] Because use of steatotic livers are actually increasing for transplantation because of a shortage of the nonsteatotic donor grafts, we should find the method for amelioration of injury in donor fatty liver at liver transplantation. A possible use of the pioglitazone treatment deserves future studies if its use for posttransplanted recipients or for nonalcoholic steatohepatitis turned out to reduce the related liver injury. This may provide a means for designing future therapeutic strategies with pioglitazone. Pioglitazone may thus be useful as a therapeutic agent for alcoholic fatty liver and merits further evaluation.

References

1. Sorensen TI, Orholm M, Bentsen KD, Hoybye G, Eghoje K, Christoffersen P. Prospective evaluation of alcohol abuse and alcoholic liver injury in men as predictors of development of cirrhosis. Lancet 1984;2:241–4.
2. Teli MR, Day CP, Burt AD, Bennett MK, James OFW. Determinants of progression to cirrhosis or fibrosis in pure alcoholic fatty liver. Lancet 1995;346:987–990.
3. Lin HA, Yang SQ, Chuckaree C, Kuhajda F, Ronnet G, Diehl AM. Metformin reverses fatty liver disease in obese, leptin-deficient mice. Nat Med 2000;6:998–1003.
4. Zhou G, Myers R, Li Y, Chen Y, Shen X, Fenyk-Melody J, Wu M, Ventre J, Doebber T, Fujii N, Musi N, Hirshman MF, Goodyear LJ, Moller DE. Role of AMP-activated protein kinase in mechanism of metformin action. J Clin Invest 2001;108:1167–1174.
5. Shimabukuro M, Zhou YT, Lee Y, Unger RH. Troglitazone lowers islet fat and restores beta cell function of Zucker Diabetic Fatty rats. J Biol Chem 1998;273:3547–3550.
6. Higa M, Zhou YT, Ravazzola M, Baetens D, Orci L, Unger RH. Troglitazone prevents mitochondrial alterations, β cell destruction, and diabetes in obese prediabetic rats. Proc Natl Acad Sci U S A 1999;96:11513–11518.
7. Kakuma T, Lee Y, Higa M, Wang ZW, Pan W, Shimomura I, Unger RH. Leptin, troglitazone, and the expression of sterol regulatory element binding proteins in liver and pancreatic islets. Proc Natl Acad Sci U S A 2000;97:8536–8541.
8. Scheen AJ. Hepatotoxicity with thiazolidinediones: is it a class effect? Drug Saf 2001;24:873–888.
9. Lieber CS, DeCarli LM, Sorrell MF. Experimental methods of ethanol administration. Hepatology 1989;10:501–510.
10. Maeshida Y, Kiyota Y, Yoshimura Y, Motohashi M, Tanayama S. Disposition of the new antidiabetic agent pioglitazone in rats, dogs, and monkeys. Arzneim.-Forsch/Drug Res 1997;47:29–35.
11. Hayakawa T, Shiraki T, Morimoto T, Shii K, Ikeda H. Pioglitazone improves insulin signaling defects in skeletal muscle from Wistar fatty (fa/fa) rats. Biochem Biophys Res Commun 1996;223:439–444.
12. Horikoshi H, Yoshioka T, Kawasaki T, Nakamura K, Matsunuma N, Yamaguchi K, Sasahara K. Troglitazone (CS-045), a new antidiabetic drug. Annu Rep Sankyo Res Lab 1994;46:1–57.
13. Tahara M, Matsumoto K, Nukiwa T, Nakamura T. Hepatocyte growth factor leads to recovery from alcohol-induced fatty liver in rats. J Clin Invest 1999;103:313–320.
14. Bachorik PS, Ross JW. National cholesterol education program recommendations for measurement of low-density lipoprotein cholesterol: executive summary. Clin Chem 1995;41:1414–1420.

15. Hatch FT, Lees RS. Practical methods for plasma lipoprotein analysis. Adv Lipid Res 1968;6:1–68.
16. Tomita K, Sato M, Kajiwara K, Tanaka M, Tamiya G, Makino S, Tomizawa M, Mizutani A, Kuwano Y, Shiina T, Ishii H, Kimura M. Gene structure and promoter for *Crad2* encoding mouse cis-retinol/3α-hydroxysterol short-chain dehydrogenase isozyme. Gene 2000;251:175–186.
17. Dunn JCY, Yarmush ML, Koebe HG, Tompkins RG. Hepatocyte function and extracellular matrix geometry: long-term culture in a sandwich configuration. FASEB J 1989;3:174–177.
18. Lawrence JM, Reckless JP. Actos (pioglitazone): a new treatment for type 2 diabetes. Hosp Med 2001;62:411–416.
19. Pelizzari CA, Khodarev NN, Gupta N, Calvin DP, Weichselbaum RR. Quantitative analysis of DNA array autoradiographs. Nucleic Acids Res 2000;28:4577–4581.
20. Tenenbaum SA, Carson CC, Lager PJ, Keene JD. Identifying mRNA subsets in messenger ribonucleoprotein complexes by using cDNA arrays. Proc Natl Acad Sci U S A 2000;97:14085–14090.
21. Okada T, Mizoi Y. Studies on the problem of blood acetaldehyde determination in man and level after alcohol intake. Jpn J Alcohol Drug Depend 1982;17:141–159.
22. Wright HM, Clish CB, Mikami T, Hauser S, Yanagi K, Hiramatsu R, Serhan CN, Spiegelman BM. A synthetic antagonist for the peroxisome proliferator-activated receptor gamma inhibits adipocyte differentiation. J Biol Chem 2000;275:1873–1877.
23. Levine JA, Harris MM, Morgan MY. Energy expenditure in chronic abuse. Eur J Clin Invest 2000;30:779–786.
24. Eaton S, Record CO, Bartlett K. Multiple biochemical effects in the pathogenesis of alcoholic fatty liver. Eur J Clin Invest 1997; 27:719–722.
25. Michalopoulos GK, Defrances MC. Liver regeneration. Science 1997;276:60–66.
26. Stuart KA, Riordan SM, Lidder S, Crostella L, Williams R, Skouteris GG. Hepatocyte growth factor/scatter factor-induced intracellular signaling. Int J Exp Pathol 2000;81:17–30.
27. Takehara T, Nakamura T. Protective effect of hepatocyte growth factor on *in vitro* hepatitis in primary cultured hepatocytes. Biomed Res 1991;12:335–338.
28. Ishiki Y, Ohnishi H, Muto Y, Matsumoto K, Nakamura T. Direct evidence that hepatocyte growth factor is a hepatotropic factor for liver regeneration and has a potent antihepatitis effect in vivo. Hepatology 1992;16:1227–1235.
29. Kaibori M, Kwon AH, Oda M, Kamiyama Y, Kitamura N, Okumura T. Hepatocyte growth factor stimulates synthesis of lipids and secretion of lipoproteins in rat hepatocytes. Hepatology 1998; 27:1354–1361.
30. Ntambi JM, Miyazaki M, Stoehr JP, Lan H, Kendziorski CM, Yandell BS, Song Y, Cohen P, Friedman JM, Attie AD. Loss of stearoyl-CoA desaturase-1 function protects mice against adiposity. Proc Natl Acad Sci U S A 2002;99:11482–11486.
31. Cohen P, Miyazaki M, Socci ND, Hagge-Greenberg A, Liedtke W, Soukas AA, Sharma R, Hudgins LC, Ntambi JM, Friedman JM. Role for stearoyl-CoA desaturase-1 in leptin-mediated weight loss. Science 2002;297:240–243.
32. Shimomura I, Shimano H, Korn BS, Bashmakov Y, Horton JD. Nuclear sterol regulatory element-binding proteins activate genes responsible for the entire program of unsaturated fatty acid biosynthesis in transgenic mouse liver. J Biol Chem 1998;273: 35299–35306.
33. You M, Fischer M, Deeg MA, Crabb DW. Ethanol induces fatty acid synthesis pathways by activation of sterol regulatory element-binding protein (SREBP). J Biol Chem 2002;277:29342–29347.
34. Sato S, Kaido T, Yamaoka S, Yoshikawa A, Arii S, Nakamura T, Niwano M, Imamura M. Hepatocyte growth factor prevents lipopolysaccharide-induced hepatic sinusoidal endothelial cell injury and intrasinusoidal fibrin deposition in rats. J Surg Res 1998; 80:194–199.
35. Letteron P, Fromenty B, Terris B, Degott C, Pessayre D. Acute and chronic hepatic steatosis lead to in vivo lipid peroxidation in mice. J Hepatol 1996;24:200–208.
36. Kyokane T, Norimizu S, Taniai H, Yamaguchi T, Takeoka S, Tsuchida E, Naito M, Nimura Y, Ishimura Y, Suematsu M. Carbon monoxide from heme catabolism protects against hepatobiliary dysfunction in endotoxin-treated rat liver. Gastroenterology 2001;120:1227–1240.
37. Hayashi S, Takamiya R, Yamaguchi T, Matsumoto K, Tojo SJ, Tamatani T, Kitajima M, Makino N, Ishimura Y, Suematsu M. Induction of heme oxygenase-1 suppresses venular leukocyte adhesion elicited by oxidative stress: role of bilirubin generated by the enzyme. Circ Res 1999;85:663–671.
38. Yamamoto Y, Nakajima M, Yamazaki H, Yokoi T. Cytotoxicity and apoptosis produced by troglitazone in human hepatoma cells. Life Sci 2001;70:471–482.
39. Imber CJ, Peter SDS, Handa A, Friend PJ. Hepatic steatosis and its relationship to transplantation. Liver Transpl 2002;8:415–423.

Received March 8, 2003. Accepted December 4, 2003.

Address reprint requests to: Hiromasa Ishii, M.D., Department of Internal Medicine, School of Medicine, Keio University, 35 Shinanomachi, Shinjuku-ku, Tokyo 160-8582, Japan. e-mail: hishii@sc.itc.keio.ac.jp; fax: (81) 3-3356-9654.

Supported by a grant from Keio University, School of Medicine, Nateglinide Memorial Toyoshima Research and Education Fund, and the 21st Century Center-Of-Excellence (COE) Program from Ministry of Education, Culture, Sports, Science, and Technology.

The authors thank T. Saito, H. Ochiai, M. Tomizawa, and E. Tokubo for technical assistance.

Available online at www.sciencedirect.com
SCIENCE DIRECT
Hepatology Research 28 (2004) 102–108
Hepatology Research
www.elsevier.com/locate/ihepcom

Ethanol upregulates pro-fibrogenic connective tissue growth factor (CTGF) gene expression in HepG2 cells via cytochrome P450 2E1-mediated ethanol oxidation

Masahiro Konishi[a,*], Shinzo Kato[a], Mikio Kajihara[a], Arthur Cederbaum[b], Hiromasa Ishii[a]

[a] *Department of Internal Medicine, Keio University School of Medicine, 35 Shinanomachi, Shinjuku-ku, Tokyo 160-8582, Japan*
[b] *Department of Biochemistry and Molecular Biology, Mount Sinai School of Medicine, New York, NY, USA*

Received 13 November 2003; received in revised form 11 December 2003; accepted 15 December 2003

Abstract

Connective tissue growth factor (CTGF) is a pro-fibrogenic molecule involved in several human fibrotic disorders. CTGF overexpression in the liver, through upregulation of CTGF mRNA in hepatic stellate cells (HSCs), is reported to correlate with the degree of fibrosis. Although alcohol is a major cause of hepatic fibrosis, the role of CTGF in alcoholic hepatic fibrogenesis, has been poorly understood. Oxidative stress, mediated by ethanol-inducible Cytochrome P-4502E1(CYP2E1), has been implicated as a crucial factor in alcoholic hepatic fibrogenesis. Therefore, we investigated the contribution of CYP2E1-mediated ethanol oxidation to CTGF mRNA expression by using a well-established HepG2 cell line constitutively expressing CYP2E1 (E9 cells). CTGF mRNA quantitation by a real-time reverse polymerase chain reaction (RT-PCR) showed a significant increase in CTGF mRNA levels in ethanol-treated E9 cells. Phorbol myristate acetate (PMA), which enhances CYP2E1 expression, increased CTGF mRNA levels. This increase was diminished after co-incubation with 4-methylpyrazole (4MP), a CYP2E1 inhibitor, or an antioxidant, *N*-acetylcysteine. We visualized the state of oxidative stress only in ethanol-treated E9 cells by a newly-established anti-acrolein-modified antibody. In conclusion, our study has first identified a possible role of CYP2E1-mediated ethanol oxidation in CTGF gene upregulation, suggesting a considerable role of CTGF in alcoholic hepatic fiberogenesis.

Keywords: Fibrosis; Oxidative Stress; Real-time RT-PCR; Acrolein

1. Introduction

Connective tissue growth factor (CTGF) is a multi-functional matricellular peptide that was originally identified from human vascular endothelial cells in culture [1]. It belongs to the CCN gene family, which includes CTGF, Cyr61/Cef10, Elm1, and Nov [2–5]. These genes are thought to exert, as immediate early growth-responsive genes, diverse cellular functions, such as cell proliferation, differentiation, apoptosis, adhesion, and embryogenesis [6,7].

CTGF mRNA and protein are over-expressed in numerous human fibrotic disorders of the lung [8], liver [6], kidney [9,10], pancreas [11], bowel [12], skin [7,13], and eyes [14]; thus its role to promote fibrosis has attracted much attention [6,7]. Hepatic fibrosis, the ultimate form of chronic liver diseases, is characterized by cell proliferation and excessive extracellular matrix (ECM) deposition [6]; in vitro, CTGF stimulates fibroblast proliferation and ECM synthesis. Recent studies, in vivo, using the liver biopsy specimens from patients with chronic viral (hepatitis B and hepatitis C) or alcoholic hepatic fibrosis revealed a significant correlation between CTGF immunostaining intensity and severity of fibrosis [6].

Transforming growth factor-β (TGF-β) not only induces collagen and ECM synthesis in the liver [7] but also regulates other biologically active pro-fibrotic mediators, such as CTGF. Indeed, the CTGF gene has a unique TGF-β-responsive element in its promoter [15]; it is conceivable that CTGF plays a role as a downstream mediator of some of the pro-fibrotic actions of TGF-β.

Hepatic stellate cells (HSCs) play a crucial role in hepatic fibrosis since these cells undergo activation with ECM deposition during firbogenesis [15–22]. TGF-β initiates activation of HSCs in culture and induces CTGF expression.

* Corresponding author. Tel.: +81-3-3353-1211x62298; fax: +81-3-3353-6247.
E-mail address: k-show@ja2.so-net.ne.jp (M. Konishi).

1386-6346/$ – see front matter © 2004 Elsevier B.V. All rights reserved.
doi:10.1016/j.hepres.2003.12.003

CTGF mRNA expression is stimulated not only by TGF-β alone but also CTGF itself in HSC T6 cells [8]. In mouse fibroblasts, CTGF mRNA expression is stimulated by TGF-β, ethanol, or acetaldehyde. Co-incubating HSCs from fa/fa rats with glucose or insulin enhances CTGF expression, independent of TGF-β actions [23]. These data, taken together, suggest both autocrine or paracrine pathways of the CTGF action on HSCs are likely since exogenous CTGF is able to modulate HSC function. Thus, the underlying mechanisms which regulate CTGF expression in other cell types as well as HSCs in the liver await further investigations.

In alcoholic hepatic fibrogenesis, induction of oxidative stress response has been implicated as one of the major driving factors [24–31]. Microsomal ethanol oxidizing system containing Cytochrome P-4502E1 (CYP2E1), an effective producer of reactive oxygen species (ROS), is strikingly inducible by chronic and excessive ethanol consumption, which results not only in an increased production of acetaldehyde but also in the generation of substantial amount of superoxide as well as hydroxy and other free radicals. In HSCs, CYP2E1 is present at levels of only 4% or less those found in hapatocytes. Therefore, CYP2E1-mediated oxidative stress as a result of chronic and excessive ethanol consumption is more centered in hapatocytes rather than in HSCs [32,33].

Cederbaum, et al developed the HepG2 cell line stably expressing CYP2E1, namely E9. By using the cultured E9 cells, we explored the impact of CYP2E1-mediated ethanol oxidation on CTGF gene expression [34–37].

2. Materials and methods

2.1. Cell lines

Two human hepatoma HepG2 sublines were established and provided by Dr. Arthur Cederbaum; HepG2-MVh2E1-9 (E9) which has been transduced to stably overexpress 2E1 (Fig. 1) and HepG2-MV-5 (MV-5) which contains only a retroviral shuttle vector lacking the human CYP2E1 complementary DNA (cDNA). MV-5 cells do not express detectable CYP2E1. The *p*-nitrophenol oxidation activity of E9 cells was measured and E9 cells were used for the experiment only when the activity was maintained at the levels of 50–100 pmol/min/mg microsomal protein. Protein concentration was determined using the modified Lowry protein assay reagent kit (PERBIO, Rockford, IL).

Both cells were grown in minimum essential medium (MEM), 10% fetal bovine serum (FBS) and 0.1 mg/ml G418, supplemented with 1% penicillin-streptomycin-neomycin antibiotics, under standard culture conditions (5% CO_2, 37 °C). Cells were subcultured at a 1:5 ratio once a week.

2.2. Cell treatment with ethanol

During the actual treatment with ethanol, 1×10^6–2×10^6 cells were seeded on each well of a 6-well plate (Iwaki Glass, Tokyo, Japan) and incubated in 5% CO_2 at 37 °C. Hepatozyme, a commercial serum-free replacement (GIBCO BRL, Rockville, MD), which supports the growth of human hepatoma cells very well, was used as a culture medium. No hepatotoxicity was noted when the cells were cultured with

Fig. 1. Cell morphology of E9 cells in culture. HepG2 cells which stably express CYP2E1 (E9 cells) after 24 h treatment with 100 mM ethanol.

hepatozyme (data not shown). For incubation with ethanol, various concentrations of ethanol and other reagents were added to the culture medium. All sample as well as control plates were wrapped with parafilm to minimize evaporation of ethanol. Culture medium and reagents were changed every 24 h. No significant changes in pH were observed in any of the samples.

2.3. Total RNA extraction and quantitative analysis using real-time reverse transcription-PCR

Total RNA from the cell lines was extracted by using RNeasy Mini Kits (QUIAGEN, Valencia, CA) according to the manufacture's protocol.

CTGF mRNA analysis was carried out by the quantitative real-time RT-PCR method; the theoretical base for this method has been described in detail elsewhere [38–40]. Real-time RT-PCR was performed using the ABI PRISM 7700 Sequence Detection System (PE Applied Biosystems, Foster City, CA). The sequence-specific oligonucleotide primers and probe used for CTGF were designed using Primer Express software 1.5 (PE Applied Biosystems, Foster City, CA), as shown below.

CTGF:

Forward 5′-AACCGCAAGATCGGCGT-3′
Reverse 5′-CCGTACCACCGAAGATGCA-3′
Probe 5′-6FAM-TGCACCGCCAAAGATGGTGCTC-TAMRA-3′

Reverse transcription was carried out with 3 mg of total RNA as template using Takara PCR (AMV) kit Ver.2.1 according to the manufacture's protocol (Takara Bio, Shiga, Japan). Each PCR sample contained 5 μl of synthesized cDNA, 12.5 μl of TaqMan 2X Universal Mix (PE Applied Biosystems, Foster City, CA), 2.5 μl of each of the gene-specific probe and primers; water was finally added to the total volume of 25 μl. Primer and TaqMan probe final concentrations in each reaction were 200 and 100 nM, respectively. The actual two-step quantitative PCR was performed as follows: 2 min at 50 °C, 10 min at 95 °C, followed by 40 cycles of 95 °C for 15 s and 60 °C for 1 min.

2.4. Oxidative stress

To verify the presence of protein-bound acrolein, a newly-established potential marker for oxidative stress in the presence or absence of ethanol, anti-acrolein-modified keyhole limpet hemocyanin (KLH) polyclonal antibody or namely mAb5F6, which was kindly provided by Dr. Koji Uchida (Nagoya University, Nagoya, Japan), was used [41,42].

Upon incubation with BSA, acrolein (CH_2=CH–CHO), a ubiquitous pollutant in the environment, was rapidly incorporated into the protein and generated the protein-linked carbonyl derivative, a putative marker of oxidatively modified protein under oxidative stress. The mAb5F6 was raised against the acrolein-modified KLH to verify the protein-bound acrolein in vivo.

The cells were plated on a type I collagen-coated chamber slide (Beckton Dickson, Bedford, MA) at a density of approximately 5×10^3 cells/cm^2 and then adhered on the substratum for 1 h at room temperature. Two hundred microliter hepatozyme, serum-free culture medium, and other reagents as described above were added and the cells were cultured for overnight in the CO_2 incubator at 37 °C. The chamber slide was rinsed three times in phosphate-buffered saline (PBS, pH 7.2) followed by fixation with 4% paraformaldehyde in PBS for 30 min. The chamber slide was then washed twice with PBS, permealized with 0.05% saponin, followed by the incubation with blocking solution (5% sheep serum in PBS) for 60 min. The cells were incubated with the primary antibody, mAb5F6 in 0.1% Triton and 1% BSA for 2 h at room temperature. The chamber slide was washed twice with PBS. The cells were incubated with the secondary antibody (FITC linked anti-mouse IgG made in Sheep) for 1 h (dilute to 1:200 in 1% BSA, 0.1% Triton).

The chamber slide was finally washed twice with PBS. The reacted preparations were examined with a confocal imaging system equipped with a krypton–argon laser (NIKON, Tokyo, Japan).

3. Results

3.1. Connective tissue growth factor (CTGF) mRNA expression in ethanol-treated HepG2 E9 cells constitutively expressing CYP2E1

To evaluate the effect of CYP2E1-mediated ethanol oxidation on CTGF mRNA expression, we used the real-time RT-PCR method for CTGF mRNA quantification. Ethanol is known to be cytotoxic in a dose- and time-dependent manner to E9 cells, which constitutively express CYP2E1 [31–33]. CYP2E1 expression was validated before each experiment by assaying for *p*-nitrophenol oxidation. E9 cells were treated with 100 mM ethanol for 24 and 48 h under serum-free conditions. As shown in Fig. 2, CTGF mRNA levels were significantly higher in ethanol-treated E9 cells at 24 h and further increased at 48 h. In contrast, no substantial increase in CTGF mRNA levels was observed in E9 cells without ethanol treatment (Fig. 2).

Phorbol myristate acetate (PMA), which enhances expression of CYP2E1, has been known to increase cytotoxicity of ethanol to E9 cells. After co-incubation for 24 h with ethanol and PMA, there was nearly a 1.6-fold increase in CTGF mRNA levels (Fig. 3) compared with E9 cells treated with 100 mM ethanol alone. PMA significantly increased CTGF mRNA levels also at 48 h. Since PMA enhanced CYP2E1 expression in E9 cells, this result suggests CYP2E1-mediated ethanol oxidation may be involved in the mechanisms of CTGF upregulation.

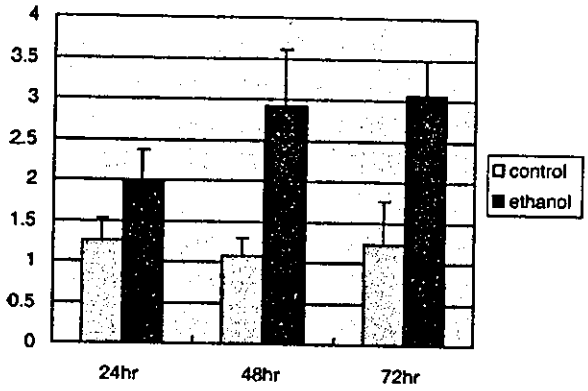

Fig. 2. Time-course effect of ethanol on CTGF mRNA expression in E9 cells. CTGF mRNA was quantified by the real-time RT-PCR method. Results were expressed as threshold cycles (Ct) standardized by Ct for housekeeping gene, GAPDH. CTGF mean mRNA levels of E9 cells ($n = 6$ for 24, 48, 72 h) in the presence or absence of 100 mM ethanol were compared ($n = 6$ for 24, 48, 72 h). At 24 h, CTGF mRNA mean level was significantly higher in ethanol-treated E9 cells than in control cells (1.98 ± 0.40 vs. 1.26 ± 0.26, $P < 0.05$). The same results were observed at 48 h (2.93 ± 0.67 vs. 1.07 ± 0.23, $P < 0.05$) and 72 h (3.05 ± 0.44 vs. 1.23 ± 0.53, $P < 0.05$). Data are expressed as means ± S.D. $P < 0.05$ vs. control.

To further clarify the mechanisms of CTGF upregulation in this cell line model, we used 4-methylpyrazole (4MP), a ligand of CYP2E1. 4MP has been used to be an effective inhibitor of CYP2E1 catalytic activity including oxidation of ethanol. 4MP moderately suppressed CTGF mRNA levels at 24 h after the addition and the significant suppression was attenuated at 48 h (Fig. 4). This result may indicate that inhibition of CYP2E1-mediated ethanol oxidation by 4MP suppressed CTGF mRNA levels.

CTGF mRNA levels in the control cell line were also quantified. MV-5 cells were transfected with only an empty viral vector. These control cells do not stably express detectable CYP2E1. Time-course experiments were carried out

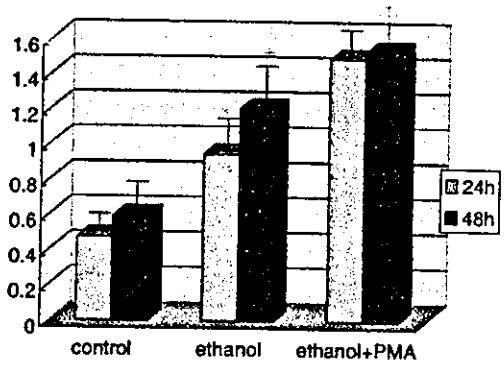

Fig. 3. CYP2E1-dependent Increase of CTGF mRNA Levels. Mean CTGF mRNA levels in E9 control cells ($n = 6$ at 24, 48 h) were compared with E9 cells ($n = 6$ at 24, 48 h) treated with 100 mM ethanol alone, 100 mM ethanol plus Phorbol 12-myrisate 13-acetate (PMA). PMA, a reagent which increases the expression of CYP2E1. PMA significantly enhanced CTGF mRNA expression in ethanol-treated E9 cells. $^{*}P < 0.05$ vs. control. $^{+}P < 0.05$ vs. E9 cells treated with 100 mM ethanol alone.

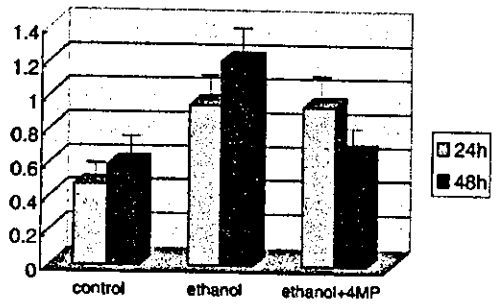

Fig. 4. 4MP, a CYP2E1 inhibitor, reduced CTGF mRNA expression. Mean CTGF mRNA values of ethanol-treated E9 cells ($n = 6$ at 24, 48 h) with and without an addition of 5 mM 4-methylpyrazole (4MP), a ligand of CYP2E1 inhibitor were compared. 4MP has been used to be an effective inhibitor of CYP2E1 catalytic activity including oxidation of ethanol. CTGF mRNA mean level was significantly lower in E9 cells treated with 100 mM ethanol plus 4MP than in E9 cells treated with 100 mM ethanol alone. $^{*}P < 0.05$ vs. control.

to evaluate the effect of ethanol on CTGF mRNA expression. Fig. 5 illustrates that ethanol induced no significant changes in CTGF mRNA levels in MV-5 cells both at 24 and 48 h. Co-incubation with ethanol and PMA induced no significant increase in CTGF mRNA levels in these control cells. Ethanol did not change CTGF mRNA levels in the presence or absence of 4MP in MV-5 cells.

Increased reactive oxygen species production by CYP2E1 metabolism of ethanol may cause CTGF mRNA upregulation in E9 cells. Fig. 6 illustrates the effects of an antioxidant on CTGF mRNA expression. We preincubated E9 cells for 6 h prior to 100 mM ethanol treatment in the presence or absence of *N*-acetylcysteine. Astonishingly, CTGF mRNA levels were reduced by 50% at 24 h and by 80% at 48 h in the presence of *N*-acetylcysteine.

3.2. Visualizing the state of oxidative stress in E9 cells in the absence or presence of ethanol

Various lines of evidence indicate that the ethanol-induced oxidative stress response in the liver plays an important role in the alcoholic liver fibrogenesis. The present study revealed

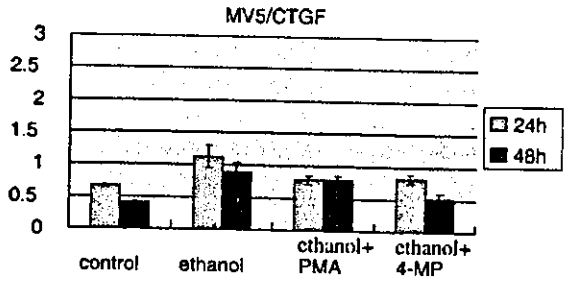

Fig. 5. No CTGF Upregulation in Control Cells. Mean CTGF mRNA levels of MV5 cells ($n = 6$ at 24 and 48 h), which have been transfected with an empty viral vector, were compared. No significant changes in CTGF mRNA levels were observed with (1) 100 mM ethanol ($n = 6$ for 24, 48 h) alone, (2) 100 mM ethanol plus PMA ($n = 6$ for 24, 48 h), or (3) 100 mM ethanol plus 4-MP ($n = 6$ for 24, 48 h).

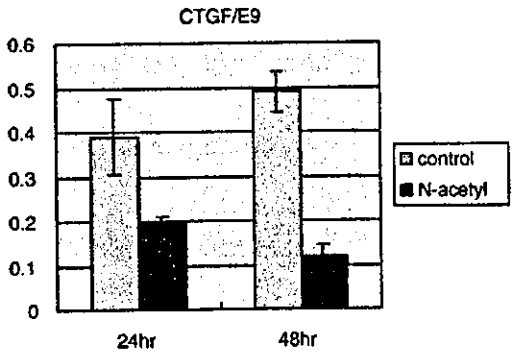

Fig. 6. N-acetylcysteine diminished CTGF Upregulation. Mean CTGF mRNA levels of E9 cells were compared incubated with (1) 100 mM ethanol ($n = 6$ for 24, 48 h) and (2) 100 mM ethanol plus 0.05 mM *N*-acetylcysteine, an inhibitor of lipid peroxidation. CTGF mRNA mean level was significantly lower in E9 cells treated with 100 mM ethanol plus *N*-acetylcysteine compared to control E9 cells treated with 100 mM ethanol alone. $P < 0.05$ vs. control.

CYP2E1 overexpression by PMA upregulated CTGF mRNA and this upregulation was noticeably diminished by an antioxidant. CYP2E1-mediated ethanol oxidation, therefore, is likely to upregulate CTGF mRNA expression.

Ethanol-treated E9 cells were examined histochemically to visualize the state of oxidative stress using anti-acrolein-modified KLH polyclonal antibody, mAb5F6. Since CTGF mRNA quantification in this cell line model was carried out at 24 h after the initial ethanol treatment, we compared E9 cells in the presence or absence of 100 mM ethanol at this time point. Fig. 7 illustrates the result of the immunohistochemical detection of protein-bound acrolein. There was no staining in E9 cells without ethanol treatment (Fig. 7a). E9 cells were stained after treatment for 24 h with 100 mM ethanol (Fig. 7b).

4. Discussion

CTGF is a profibrogenic molecule involved in several human fibrotic disorders including alcoholic hepatic fibrosis. CTGF has attracted much attention as a potential target of future antifibrotic therapies since inhibition of CTGF actions might specifically block profibrotic effects of TGF-β, without affecting anti-proliferative and immunosuppressive effects of TGF-β. Since alcohol is a leading cause of hepatic fibrosis in most Western countries with high morbidity and mortality, the role of CTGF in alcoholic hepatic fibrogenesis should be defined. Our study has first identified a major role of CYP2E1-mediated ethanol oxidation in CTGF gene regulation by using a well-established cell culture model. Indeed, correlation between induction of CYP2E1, lipid peroxidation, and ethanol-induced liver injury has been reported with the continuous intragastric infusion model of ethanol feeding [29,43,44]. Induction of CYP2E1 and the formation of reactive intermediates, such as reactive oxygen species and lipid peroxidation, is one of the central mechanisms by which ethanol becomes hepatotoxic. Our data simply demonstrated that ethanol alone did not upregulate CTGF expression and

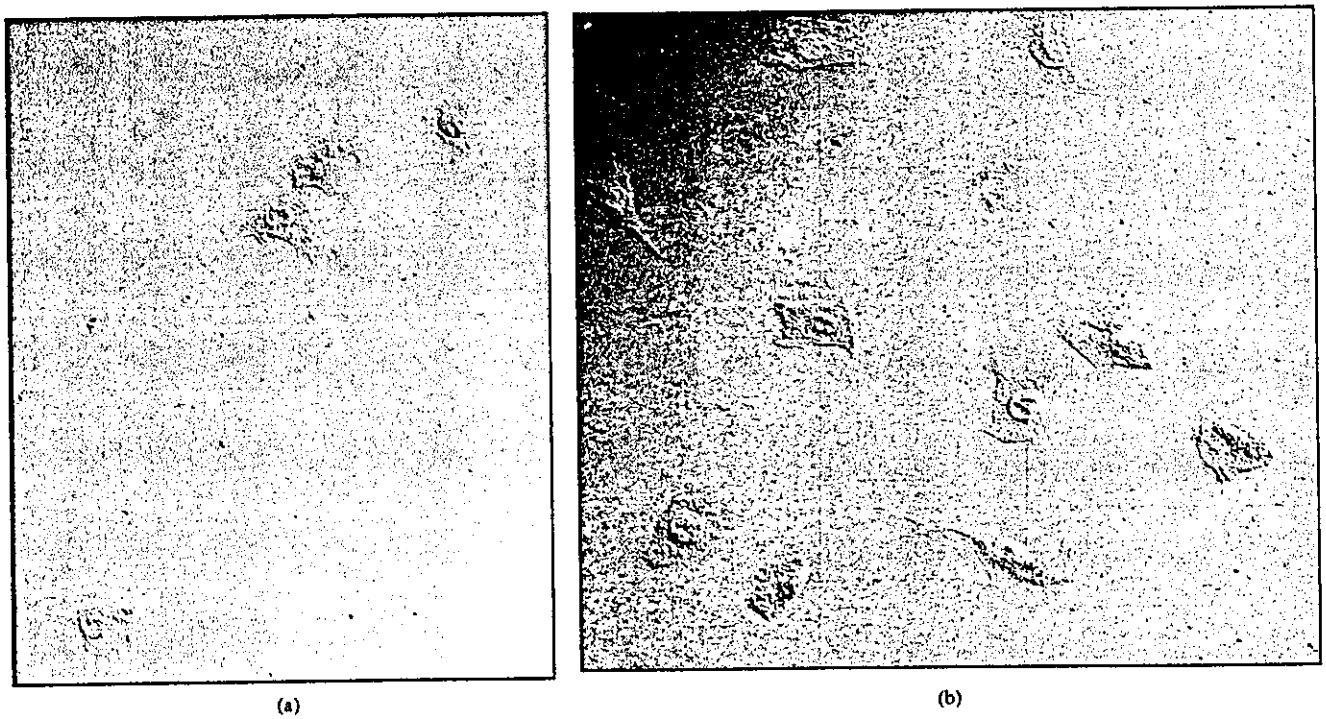

Fig. 7. Immunohistochemical detection of protein-bound acrolein, a novel marker for oxidative stress. E9 cells untreated (a) and treated with 100 mM ethanol for 24 h (b) were immunostained with anti-acrolein-modified KLH polyclonal antibody, mAb5F6. Only ethanol-treated E9 cells were positive. (original magnification: 200×).

CTGF upregulation seemed to be correlated with and dependent upon the degree of ethanol-inducible CYP2E1 expression. Due to the fact that an antioxidant diminished CTGF upregulation and only ethanol-treated E9 cells were positive for mAb5F6, a putative maker for oxidative stress, CYP2E1-mediated oxidative stress may directly upregulate CTGF expression in alcoholic hepatic fibrogenesis.

Earlier studies on CTGF established a firm relationship between TGF-β actions and CTGF expression [15,18]. TGF-β induces CTGF through different signaling pathways as well as a specific TGF-β responsive element in the CTGF promoter [15]. CTGF may function as a downstream mediator of TGF-β and share some of the fibrogenic actions including the fibroblast proliferation and ECM synthesis [6,15,18,25]. However, exogenous CTGF produced in other cells of the liver and its function to modulate HSC actions has become relevant. Moreover, the existence of TGF-β-independent signaling pathways of CTGF, has also been verified [27]. In our cell culture model, CTGF was produced in transformed hepatocytes, independent of TGF-β actions, since TGF-β was expressed at minimal levels in this cell line even after incubation with 100 mM ethanol (data not shown). Although the relative importance of exogenous CTGF in the activation process of HSCs remains uncertain, CYP2E1-mediated ethanol oxidation may be directly involved in CTGF upregulation in hepatocytes.

The whole regulation processes of liver fibrogenesis, however, are very complex and seem to require activation of signaling pathways of numerous cytokines and growth factors [45]. In ALD, there is a sizable portion of cases with fibrosis without alcoholic hepatitis. A study in the UK [46] has suggested in alcoholic hepatic fibrosis, neither necroinflammation nor an increase in Kupffer cells is an absolute prerequisite for HSC activation and subsequent fibrosis. Since CTGF upregulation in our transformed hapatocytes seems to depend more upon the degree of CYP2E1-mediated ethanol oxidation rather than the degree of inflammation in the liver, it may be concluded that our study provides evidence in part that CTGF is one of the intracellular pro-fibrogenic molecules, mediating activation and proliferation of HSCs in alcoholic hepatic fibrogenesis.

Acknowledgements

The authors thank Dr. Defeng Wu of Mount Sinai School of Medicine for providing technical supports and fruitful discussions.

References

[1] Bradham DM, Igarashi A, Potter RL, Grotendorst GR. Connective tissue growth factor: a cysteine-rich mitogen secreted by human vascular endothelial cells is related to the SRC-induced immediate early gene product CEF-10. J Cell Biol 1991;114:1285–94.

[2] Simmons DL, Levy DB, Yannoni Y, Erikson RL. Identification of a phorbol ester-repressible v-src-inducible gene. Proc Natl Acad Sci 1989;86:1178–82.

[3] O'Brien TP, Yang GP, Sanders L, Lay LF. Expression of Cyr 61, a growth factor inducible immediate early gene. Mol Cell Biol 1990;10:3569–77.

[4] Ryseck RP, MacDonald-Bravo H, Mattei MG, Bravo R. Mapping and expression of Fisp-12, a growth factor inducible gene encoding a cystein-rich protein. Cell Growth Differ 1991;2:225–33.

[5] Joliot V, Martinerie C, Dambrine G, Plassiart G, Brisac M, Crochet J, et al. Proviral rearrangements and overexpression of a new cellular gene (nov) in myeloblastosis-associated virus type 1-induced nephroblastomas. Mol Cell Biol 1992;12:10–21.

[6] Paradis V, Dargere D, Vidaud M, De Gouville AC, Huet S, Martinez V, et al. Expression of connective tissue growth factor in experimental and human liver fibrosis. Hepatology 1999;30:968–76.

[7] Igarashi A, Okochi H, Bradham DM, Grotendorst GR. Regulation of connective tissue growth factor gene expression in human skin fibroblasts and during wound repair. Mol Biol Cell 1993;4:637–45.

[8] Lasky JA, Ortiz LA, Tonthat B, Hoyle GW, Corti M, Athas G, et al. Connective tissue growth factor mRNA expression is upregulated in bleomycin-induced lung fibrosis. Am J Physiol 1998;275:L365–71.

[9] Ito Y, Aten J, Bende RJ, Oemar BS, Rabelink TJ, Weening JJ, et al. Expression of connective tissue growth factor in human renal fibrosis. Kidney Int 1998;53:853–61.

[10] Ito Y, Goldschmeding R, Bende RJ, Claessen N, Anwar Chand M, Kleij L, et al. Kinetics of connective tissue growth factor expression during experimental proliferative glomerulonephritis. J Am Soc Nephrol 2001;12:472–84.

[11] di Mola FF, Friess H, Martignoni ME, et al. Connective tissue growth factor is involved in pancreatic repair and tissue remodeling in human and rat acute necrotizing pancreatitis. Ann Surg 2002;235:6–70.

[12] Dammeier J, Brauchle M, Falk W, Grotendorst GR, Werner S. Connective tissue growth factor: a novel regulator of mucosal repair and fibrosis in inflammatory bowel disease? Int J Biochem Cell Biol 1998;30(8):909–22.

[13] Igarashi A, Nashiro K, Kikuchi K, Sato S, Ihn H, Fujimoto M, et al. Connective tissue growth factor gene expression in tissue sections from localized scleroderma, keloid, and other fibrotic skin disorders. J Invest Dermatol 1996;106:729–33.

[14] van Setten GB, Blalock TD, Grotendorst G, Schultz GS. Detection of connective growth factor(CTGF) in human tear fluid: preliminary results. Acta Ophthalmol Scand 2003;81(1):51–3.

[15] Grotendorst GR, Okochi H, Hayashi N. A novel transforming growth factor beta response element controls the expression of the connective tissue growth factor gene. Cell Growth Differ 1996;7:469–80.

[16] Frazier K, Williams S, Kothapalli D, Klapper H, Grotendorst GR. Stimulation of fibroblast cell growth, matrix production, and granulation tissue formation by connective tissue growth factor. J Invest Dermatol 1996;107:404–11.

[17] Kreeva ML, Latinkic BV, Kolesnikova TV, Chen CC, Yang GP, Abler AS, et al. *Cyr*61 and *Fisp*12 are both ECM-associated signaling molecules: activities, metabolism, and localization during development. Exp Cell Res 1997;25:63–77.

[18] Grotendorst GR, Okochi H, Hayashi N. A novel transforming growth factor beta response element controls the expression of the connective tissue growth factor gene. Cell Growth Differ 1996;7:469–80.

[19] Friedman SL, Roll FJ, Boyles, Bissell DM. Hepatic lipocytes: the principal collagen-producing cells of normal rat liver. Proc Natl Acad Sci 1985;82:8681–8685.

[20] Friedman SL. Stellate cell activation in alcoholic fibrosis—an overview. Alcohol Clin Exp Res 1999;23:904–10.

[21] Friedman SL. Molecular regulation of hepatic fibrosis, an integrated cellular response to tissue injury. J Biol Chem 2000;275:2247–50.

[22] Hautekeete ML, Geerts A. The hepatic stellate (Ito) cell: its role in human liver disease. Virchows Arch 1997;430:195–207.

[23] Williams EJ, Arthur MJP, Benyon RC. Increased expression of connective tissue growth factor in fibrotic human liver and activated hepatic stellate cells [Abstract]. Hepatology 1998;28: 300A.
[24] Williams EJ, Gaca MD, Brigstock DR, Arthur MJ, Benyon RC. Increased expression of connective tissue growth factor in fibrotic human liver and in activated hepatic stellate cells. J Hepatol 2000;32: 754–61.
[25] Rachfal AW, Brigstock DR. Connective tissue growth factor (CTGF/CCN2) in hepatic fibrosis. Hepatol Res 2003;26(1):1–9.
[26] Frazier K, Williams S, Kothapalli D, Klapper H, Grotendorst GR. Stimulation of fibroblast cell growth, matrix production, and granulation tissue formation by connective tissue growth factor. J Invest Dermatol 1996;107:404–11.
[27] Paradis V, Perlemuter G, Bonvoust F, Dargere D, Parfait B, Vidaud M, et al. High glucose and hyperinsulinemia stimulate connective tissue growth factor expression: a potential mechanism involved in progression to fibrosis in nonalcoholic steatohepatitis. Hepatology 2001;34:738–44.
[28] Ekstrom G, Ingelman-Sundberg M. Rat liver microsomal NADPH-supported oxidase activity and lipid peroxidation dependent on ethanol-inducible cytochrome P-450 (P-450IIE1). Biochem Pharmacol 1989;38:1313–8.
[29] Tsukamoto H. Oxidative stress, antioxidants, and alcoholic liver fibrogenesis. Alcohol 1993;10:465–7.
[30] Poli G, Parola M. Oxidative damage and fibrogenesis. Free Rad Biol Med 1997;22:287–305.
[31] Kamimura S, Gaal K, Britton RS, Bacon BR, Triadafilopoulos G, Tsukamoto H. Increased 4-hydroxynonenal levels in experimental alcoholic liver disease: association of lipid peroxidation with liver fibrogenesis. Hepatology 1992;16:448–53.
[32] Oinonen T, Koivisto T, Lindros KO. No significant expression of CYP2E1 in rat stellate cells. Biochem Pharmacol 1998;56(8): 1075–8.
[33] Casini A, Pellegrini G, Ceni E, Salzano R, Parola M, Robino G, et al. Human hepatic stellate cells express class I alcohol dehydrogenase and aldehyde dehydrogenase but not cytochrome P4502E1. J Hepatol 1998;28(1):40–5.
[34] Wu D, Cederbaum AI. Ethanol-induced apoptosis to stable HepG2 cell line expressing cytochrome P-4502E1. Alcohol Clin Exp Res 1999;23(1):67–76.
[35] Mari M, Wu D, Nieto N, Cederbaum AI. CYP2E1-dependent toxicity and up-regulation of antioxidant genes. J Biomed Sci 2001;8:52–8.
[36] Wu D, Cederbaum AI. Ethanol cytotoxicity to a transfected HepG2 cell line expressing human cytochrome P4502E1. J Biol Chem 1996;271:23914–9.
[37] Chen Q, Galleano M, Cederbaum AI. Cytotoxicity and apoptosis produced by arachidonic acid in HepG2 cells overexpressing human cytochrome P4502E1. J Biol Chem 1997;272:14532–41.
[38] Heid CA, Stevens J, Livak KJ, Williams PM. Real time quantitative PCR. Genome Res 1996;6:986–94.
[39] Gibson UEM, Heid CA, Willaims PM. A novel method for real time quantitative RT-PCR. Genome Res 1996;6:995–1000.
[40] Bieche I, Laurendeau I, Tozlu S, Olivi M, Vidaud D, Lidereau R, et al. Quantitation of myc gene expression in sporadic breast tumors with a real-time reverse transcription-PCR assay. Cancer Res 1999;59: 2759–65.
[41] Uchida K, Kanematsu M, Sakai K, Matsuda T, Hattori N, Mizuno Y, et al. Protein-bound acrolein: potential markers for oxidative stress. Proc Natl Acad Sci 1998;95:4882–7.
[42] Uchida K, Kanematsu M, Morimitsu Y, Osawa T, Noguchi N, Niki N. Acrolein is a product of lipid peroxidation reaction. Formation of free acrolein and its conjugate with lysine residues in oxidized low-density lipoproteins. J Biol Chem 1998;273:16058–66.
[43] Morimoto M, Hagbjork AL, Nanji AA, et al. Role of cytochrome P45022E1 in alcoholic liver disease pathogenesis. Alcohol 1993;10(6):459–64.
[44] French SW. Biochemistry of alcoholic liver disease. Crit Rev Clin Lab Sci 1992;29(2):83–115.
[45] Chenn MM, Lam A, Abraham JA, Schreiner GF, Joly AH. CTGF expression is induced by TGF-β in cardiac fibroblasts and cardiac myocytes: a potential role in heart fibrosis. J Mol Cell Cardiol 2000;32:1805–19.
[46] Reeves HL, Burt AD, Wood S, Day CP. Hepatic stellate cell activation occurs in the absence of hepatitis in alcoholic liver disease and correlates with the severity of steatosis. J Hepatol 1996;25:677–83.

Bax interacts with the voltage-dependent anion channel and mediates ethanol-induced apoptosis in rat hepatocytes

Masayuki Adachi, Hajime Higuchi, Soichiro Miura, Toshifumi Azuma, Sayaka Inokuchi, Hidetsugu Saito, Shinzo Kato and Hiromasa Ishii

AJP - GI 287:695-705, 2004. First published Mar 25, 2004; doi:10.1152/ajpgi.00415.2003

AJP - Gastrointestinal and Liver Physiology publishes original articles pertaining to all aspects of research involving normal or abnormal function of the gastrointestinal tract, hepatobiliary system, and pancreas. It is published 12 times a year (monthly) by the American Physiological Society, 9650 Rockville Pike, Bethesda MD 20814-3991. ISSN: 0193-1857, ESSN: 1522-1547. Visit our website at http://www.the-aps.org/.

Am J Physiol Gastrointest Liver Physiol 287: G695–G705, 2004.
First published March 25, 2004; 10.1152/ajpgi.00415.2003.

Bax interacts with the voltage-dependent anion channel and mediates ethanol-induced apoptosis in rat hepatocytes

Masayuki Adachi,[1] Hajime Higuchi,[1] Soichiro Miura,[2] Toshifumi Azuma,[1] Sayaka Inokuchi,[1] Hidetsugu Saito,[1] Shinzo Kato,[1] and Hiromasa Ishii[1]

[1]*Department of Internal Medicine, Keio University School of Medicine, Shinjuku-ku, Tokyo, 160-8582; and* [2]*Second Department of Internal Medicine, National Defense Medical College, Tokorozawa, Saitama, 359-8513, Japan*

Submitted 24 September 2003; accepted in final form 22 March 2004

Adachi, Masayuki, Hajime Higuchi, Soichiro Miura, Toshifumi Azuma, Sayaka Inokuchi, Hidetsugu Saito, Shinzo Kato, and Hiromasa Ishii. Bax interacts with the voltage-dependent anion channel and mediates ethanol-induced apoptosis in rat hepatocytes. *Am J Physiol Gastrointest Liver Physiol* 287: G695–G705, 2004. First published March 25, 2004; 10.1152/ajpgi.00415.2003.—Acute ethanol exposure induces oxidative stress and apoptosis in primary rat hepatocytes. Previous data indicate that the mitochondrial permeability transition (MPT) is essential for ethanol-induced apoptosis. However, the mechanism by which ethanol induces the MPT remains unclear. In this study, we investigated the role of Bax, a proapoptotic Bcl-2 family protein, in acute ethanol-induced hepatocyte apoptosis. We found that Bax translocates from the cytosol to mitochondria before mitochondrial cytochrome *c* release. Bax translocation was oxidative stress dependent. Mitochondrial Bax formed a protein complex with the mitochondrial voltage-dependent anion channel (VDAC). Prevention of Bax-VDAC interactions by a microinjection of anti-VDAC antibody effectively prevented hepatocyte apoptosis by ethanol. In conclusion, these data suggest that Bax translocation from the cytosol to mitochondria leads to the subsequent formation of a Bax-VDAC complex that plays a crucial role in acute ethanol-induced hepatocyte apoptosis.

alcoholic liver disease; mitochondria; oxidative stress; cytochrome *c*

HEPATOCYTE APOPTOSIS IS RECOGNIZED in the liver of both clinical (19, 30) and experimental (2, 9) alcohol-related injury and is currently identified as a common feature of alcoholic liver disease. Although both oxidative stress and cytokines, i.e., TNF-α or transforming growth factor-β, have been suggested as crucial mediators of hepatocyte apoptosis in alcoholic liver disease (15, 18, 28), relatively little is known regarding the intracellular mechanisms by which ethanol induces hepatocyte apoptosis. Our previous studies demonstrated that short-term ethanol intoxication causes oxidative stress, mitochondrial dysfunction (21), and apoptosis (12, 22) in primary cultured rat hepatocytes. In these studies, ethanol induced oxidative stress by an alcohol dehydrogenase-dependent mechanism (21) and was associated with loss of the mitochondrial membrane potential ($\Delta\psi$). This loss of $\Delta\psi$ signified a change in the mitochondrial inner membrane permeability (22) and was associated with cytochrome *c* release into the cytosol (12). Cytochrome *c* may bind to apoptosis-activating factor-1 and procaspase-9, resulting in activation of caspase-9, followed by activation of effector caspase-3, -6, and -7 (34, 39). Indeed, we observed both caspase-3 and -9 activation in ethanol-treated hepatocytes, whereas activation of caspase-8 or Bid was not detected (12). Thus mitochondrial dysfunction, such as cytochrome *c* release, may initiate ethanol-induced hepatocyte apoptosis. However, the exact mechanisms responsible for the cytochrome *c* release by acute ethanol cytotoxicity are unclear.

Permeability of the inner mitochondrial membrane is regulated by the permeability transition pore (PTP) (3, 42). The exact nature of the PTP remains in dispute. One model suggests that the PTP is comprised of the outer membrane protein voltage-dependent anion channel (VDAC), the inner membrane protein adenine nucleotide translocator (ANT), and cyclophillin-D at outer and inner membrane contact sites (4). Although opening of the PTP is transient and does not cause swelling (14, 32), sustained opening of the PTP might cause mitochondrial swelling with secondary rupture of the outer membrane (31). This rupture of outer membrane leads to massive cytochrome *c* release that has been noted in both apoptotic and necrotic cell death (24). We previously reported (3) that ethanol-induced cytochrome *c* release and apoptosis were blocked by cyclosporin A (CsA), an inhibitor of the PTP component cylophillin-D, suggesting that ethanol-induced cytochrome *c* release is PTP dependent. However, the mechanism by which ethanol induces the PTP opening remains to be elucidated. Recently, the role of proapoptotic Bcl-2 family proteins in mediating the mitochondrial permeability pore has been suggested (10, 38). Therefore, we hypothesized that Bcl-2-related proteins may contribute to cytochrome *c* release during alcohol cytotoxicity.

Bax and Bak, proapoptotic members of the Bcl-2 family, are crucial for apoptosis (8). Bax translocates from the cytosol to the mitochondrial outer membrane in many models of apoptosis (7). Bax inserts into the mitochondrial outer membrane on apoptotic stimuli (13, 40). Bax homotypic complex or heterotypic complex with Bak promote cytochrome *c* release from the intermembrane space of mitochondria into the cytosol (17). An in vitro study has shown that treatment of liposomes with Bax permeabilizes lipid membranes, allowing translocation of cytochrome *c* from the liposomes into the media and suggesting homotypic oligomerized channel formation composed of at least four Bax molecules (33). On the other hand, heterotypic interactions of Bax with the PTP components VDAC (29) or ANT (25) have also been suggested. Therefore, Bax may regulate VDAC or ANT function via direct molecular interactions. Interestingly, Bax-VDAC heterotypic interactions can form a large pore that is permeable to cytochrome *c* (35). The

Address for reprint requests and other correspondence: H. Ishii, Dept. of Internal Medicine, School of Medicine, Keio Univ., 35 Shinanomachi, Shinjuku-ku, Tokyo, 160-8582, Japan.

The costs of publication of this article were defrayed in part by the payment of page charges. The article must therefore be hereby marked "*advertisement*" in accordance with 18 U.S.C. Section 1734 solely to indicate this fact.

conductance of Bax-VDAC channel was calculated as 4-fold and 10-fold greater than that of VDAC or Bax homotypic channels (35).

The overall objective of the present study was to examine the mechanisms by which acute ethanol intoxication induces mitochondrial cytochrome *c* release and apoptosis. To address this objective, we formulated the following questions: *1*) Does Bax translocate from the cytosol to mitochondria on acute ethanol treatment? *2*) Is Bax translocation oxidative stress dependent? *3*) Does Bax form a complex by either homotypic oligomerization or heterotypic interactions with VDAC? *4*) Are the Bax-VDAC interactions essential for ethanol-induced apoptosis? and *5*) Is Bax-VDAC complex formation cyclosporin-A dependent? To assess these questions, rat primary hepatocytes were used in this study. Hepatocytes were treated with ethanol (50 mM), a sufficient concentration to induce apoptosis as established in previous studies (12, 22).

MATERIALS AND METHODS

Materials and reagents. Anti-human VDAC monoclonal antibody (31HL) was purchased from Calbiochem-Novabiochem (La Jolla, CA). Rabbit anti-VDAC antibody for microinjection was kindly provided by Dr. S. Shimizu (Osaka University, Osaka, Japan). Mouse anti-Bax and rabbit anti-Bax polyclonal antibodies were from Pharmingen (Eugene, OR). CsA, *N*-acetyl-cysteine (NAC), and actinomycin D (ActD) were purchased from Sigma (St. Louis, MO). Recombinant mouse TNF-α was purchased from R&D Systems (Minneapolis, MN). *N',N'*-dimethylthiourea (DMTU) was purchased from Janssen Chimica (cat. no. B-2440; Geer, Belgium). 2',7'-Dichlorofluorescin diacetate (DCFH-DA), 5-(and-6-chloromethyl-2',7'-dichlorofluorescein diacetate (CM-H_2DCFDA) Hoechst 33342, and MitoTracker Red CMXRos were purchased from Molecular Probes (Eugene, OR). Green fluorescent protein (GFP) was purchased from BD Biosciences Clontech (Palo Alto, CA).

Experimental protocol. Male Wistar rats with an average body weight of 250–300 g were used for the cell preparation. All animals received humane care in compliance with the National Research Council's criteria for humane care as outlined in "Guide for the Care and Use of Laboratory Animals" prepared by the National Academy of Science and published by the National Institutes of Health. Rat hepatocytes were isolated and cultured as previously described (6). The viability of isolated cells was >95% as determined by the trypan blue dye exclusion test. Cells were seeded on culture dishes at a concentration of 5×10^6 cells/cm^2 and incubated in DMEM (Sigma) containing 10% fetal calf serum (Invitrogen, Carlsbad, CA) for 24 h at 37°C in 5% CO_2. Every precaution was taken to ensure that the additives, medium, and plastic materials used were free of endotoxin as determined by the Limulus Amebocyte Lysate Test Kit (Whittaker Bioproducts, Walkersville, MD), which has a sensitivity of 0.1 ng/ml. Rat hepatocytes were cultured for 24 h after isolation before ethanol (50 mM) exposure. This concentration of ethanol (50 mM), which is known to be toxicologically relevant, is sufficient to induce apoptosis in cultured rat hepatocytes (22). To compare the apoptotic machineries between ethanol and TNF-related apoptotic models, TNF-α (30 ng/ml) plus ActD (0.2 μM) were exposed to hepatocytes. ActD was added to cultured hepatocytes 1 h before being added to TNF-α. In some experiments, the PTP inhibitor CsA (10 μM); the antioxidant NAC (5 mM) or DMTU (10 mM); a small, permeable, and relatively nontoxic scavenger of hydrogen peroxide; and the hydroxyl radical were added to the culture medium before treatment with ethanol or TNF-α plus ActD.

Determination of reactive oxygen species. To investigate subcellular localization of oxidative stress in hepatocytes, DCFH-DA was used according to the methods of Cathcart et al. (5) with minor modification (23). Briefly, cultured rat hepatocytes on 35-mm glass-bottom Microwell culture dishes (MatTek, Ashland, MA) were incubated with DMEM (pH 7.4) containing 1 μM DCFH-DA for 30 min at 37°C in the dark. The cells were washed three times with phenol red-free DMEM to remove the extracellular fluorescence and were observed on an inverted fluorescence microscope (Diaphot TMD-2S; Nikon, Tokyo, Japan). Mitochondria were labeled by incubation of hepatocytes with 200 nM of MitoTracker Red CMXRos. A PlanApochromat ×63 oil immersion objective and laser scanning confocal microscope system (Zeiss 410; Zeiss, Thornwood, NY) were used for visualization. Confocal images of 2'7'-dichlorofluorescein (DCF; an oxidized form of DCFH) fluorescence was collected by using a 488-nm excitation light from an argon/krypton laser, a 560-nm dichroic mirror, and a 500- to 550-nm band-pass barrier filter. Images of MitoTracker Red fluorescence were collected by using 568-nm excitation light from the argon/krypton laser, a 560-nm dichroic mirror, and a 590-nm long-pass filter. The intracellular formation of reactive oxygen species (ROS) was measured by using CM-H_2DCFDA. Cells (2×10^5 cells) were harvested in 24-well culture plates (Corning, Acton, MA) and loaded with 1 μM CM-H_2DCFDA for 30 min at 37°C. After free probes were washed with Hanks' balanced salt solution (Invitrogen, Carlsbad, CA), fluorescence was analyzed before and after ethanol treatment (20 min) under fluorescent plate reader (FLUOstar OPTIMA; BMG Labtechnologies, Durham, NC). ROS production was expressed as ROS generation equivalent to H_2O_2 (μmol/l) exposure for 10 min determined from an H_2O_2 standard, which was obtained from a fluorescence intensity from 2×10^5 cells exposed to 10–1000 μM of H_2O_2 for 10 min.

Immunocytochemistry of Bax. Hepatocytes were cultured on glass chamber slides (LAB-TEK; Nalge Nunc, Hanover Park, IL) and incubated with ethanol. MitoTracker Red was used for mitochondrial labeling as described in *Determination of reactive oxygen species*. After being washed with PBS three times, cells were fixed for 5 min using 4% paraformaldehyde in PBS and then permeabilized with 0.1% Triton X for 5 min. After being blocked with 10% fetal calf serum, cells were incubated with 1:100 dilution of rabbit anti-Bax polyclonal antibody (13686E) for 2 h at 37°C. After being washed three times, cells were incubated for 30 min with 1:250 dilution of an Oregon Green-conjugated goat anti-rabbit secondary antibody (Molecular Probes) for 45 min at 37°C. Fluorescence images were visualized by using confocal microscopy.

Preparation of protein extracts. Hepatocytes cultured on 90-mm culture dishes (Asahi Techno Glass, Tokyo, Japan) were collected by centrifugation and washed with ice-cold PBS. Cells were resuspended in 5 vol of extraction buffer (in mM: 250 sucrose, 20 HEPES pH 7.5, 1.5 $MgCl_2$, 10 KCl, 1 sodium-EDTA, 1 sodium-EGTA, 1 dithiothreitol, 0.1 PMSF, with 10 μg/ml leupeptin and 10 μg/ml aprotinin), incubated for 30 min on ice, and lysed by homogenization with 10 strokes of a Teflon homogenizer. Homogenates were centrifuged at 750 *g* for 10 min to remove cell debris. The supernatants were transferred to a fresh tube and centrifuged at 10,000 *g* for 15 min to pellet the mitochondria. The pellet (mitochondria) was resuspended in RIPA buffer (50 mM Tris·HCl, 150 mM NaCl, 1% Nonidet P-40, 0.5% deoxycholate, 0.1% SDS). The supernatants were then centrifuged at 100,000 *g*, and the resulting supernatants were designated as the cytosolic fraction (S-100). Cytosolic and mitochondrial fractions were used for immunoblot analysis. Protein concentration was determined by the bicinchoninic acid assay using BSA as the standard.

Immunoblotting. Immunoblotting for cytochrome *c* was performed by using the cytosolic S-100 fraction. Immunoblotting for Bax was performed by using mitochondrial or whole cell lysates from hepatocytes. Samples were resuspended in 20 μl of SDS-sample buffer and boiled at 90°C for 2 min, separated by 12% SDS-PAGE, and transferred to PVDF membranes (Immobilin-P; Millipore, Bedford, MA). After being blocked with 1% wt/vol skim milk and 3% wt/vol BSA in 20 mM Tris, 0.5 M NaCl, and 0.05% Tween 20, pH 7.0, for 30 min, membranes were incubated for 60 min with the primary antibodies:

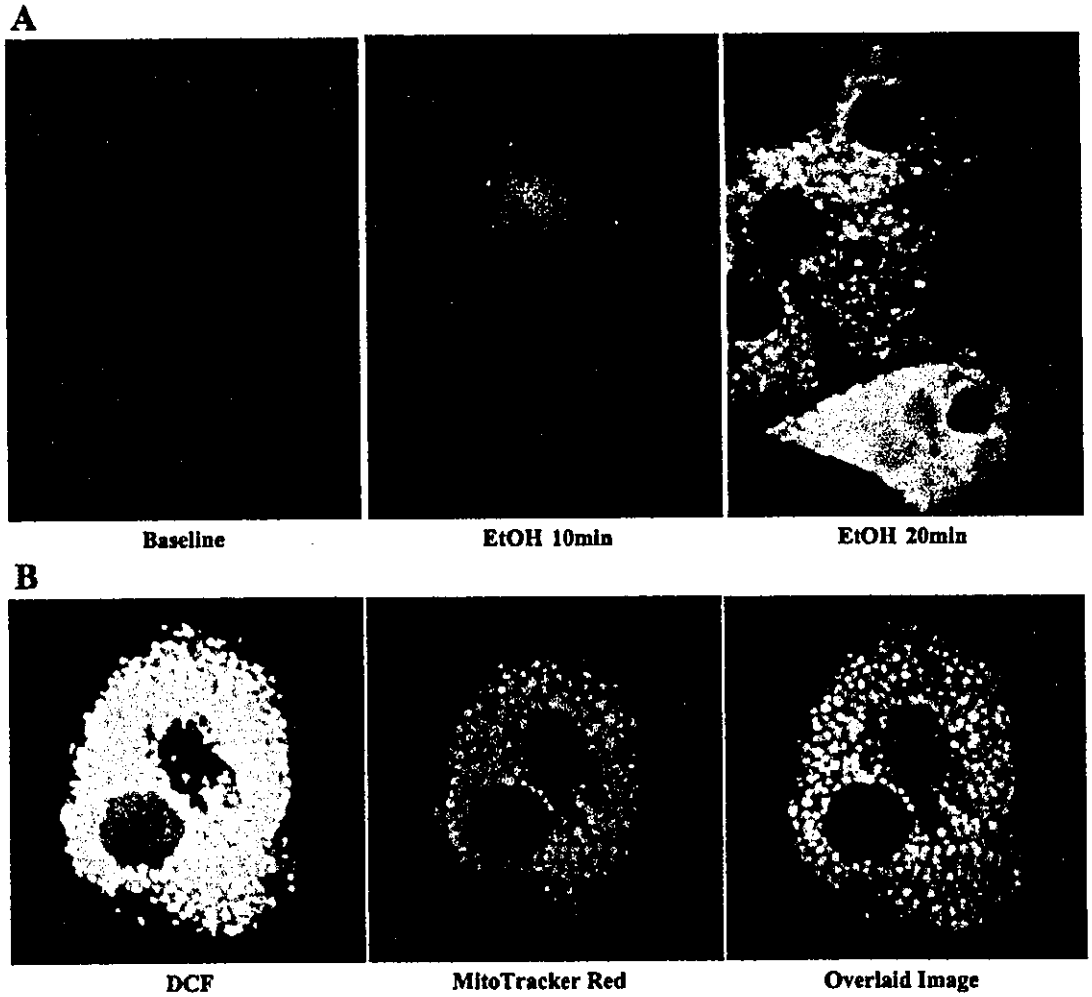

Fig. 1. Ethanol (EtOH)-induced 2′7′-dichlorofluorescein (DCF) oxidation was observed predominantly in mitochondria. Rat primary hepatocytes were incubated in the presence of 2′,7′-dichlorofluorescin diacetate (DCFH-DA; 1 μM) for 30 min. After being washed, cells were incubated with or without EtOH (50 mM). *A*: representative imaging of DCF fluorescence by fluorescent microscopy. DCF fluorescence increased in rat hepatocytes exposed to EtOH within 10 min and further increased in 20 min. *B*: hepatocytes were double-stained with MitoTracker Red CMXRos and DCFH-DA and observed by confocal microscopy. DCF-associated green fluorescence, MitoTracker Red-associated red fluorescence, and overlaid image are shown. Note that DCF fluorescence is colocalized with the MitoTracker Red fluorescence.

mouse anti-Bax (1:500 dilution) or mouse anti-cytochrome *c* (1:1,000 dilution). After being washed three times, membranes were further incubated for 60 min with peroxidase-conjugated goat anti-mouse IgG secondary antibodies (1:3,000 dilution) (Amersham, Arlington Heights, IL). Bound antibodies were detected by using enhanced chemiluminescent substrate (Amersham) and exposed to Kodak X-OMAT film. Results were confirmed by triplicate analysis.

In vivo protein cross-linking and immunoprecipitation. In vivo cross-linking for identifying Bax oligomerization or Bax-VDAC interactions was performed as described previously (1, 29). Briefly, we used the cross-linkers bis-(sulfosuccinimidyl)suberate (BS^3) and disuccinimidyl suberate (DSS) (Pierce Chemical, Rockford, IL) for Bax oligomerization or 3,3′-dithio-bis(succinimidylproprionate) (DSP) and dimethyl 3,3′-dithio-bis(proprionate)·2HCl (DTBP) (Pierce Chemical) for Bax-VDAC interaction, respectively. Cells were treated with 2 mM of cross-linkers in PBS for 30 min at room temperature. After the reaction was quenched with 50 mM Tris·HCl for 10 min at 4°C, cells were washed in PBS. Cells were then lysed with lysis buffer (in mM: 10 Tris·HCl, pH 7.4, 142.5 KCl, 5 $MgCl_2$, 1 EDTA, 1 PMSF, with 0.5% Nonidet P-40, and 20 μM leupeptin) for 30 min on ice and centrifuged to remove insoluble debris.

Immunoprecipitation was carried out as follows. Samples were precleared by mixing with 50 μl of 50% (vol/vol) protein G-Sepharose beads for 60 min at 4°C, and the beads were removed by centrifugation. The resultant supernatants were incubated with appropriate antibodies (2 μg/ml) at 4°C for 2 h. Immunoprecipitates were collected by incubating with protein G-Sepharose for 60 min, followed by centrifugation for 2 min at 4°C. The pellets were washed with lysis buffer three times. After the final wash, the beads were suspended in SDS-sample buffer, and the samples were analyzed by SDS-PAGE and Western blotting as described in *Immunoblotting*.

Microinjection. Microinjection was performed by using a micromanipulator (Narishige, Tokyo, Japan) as described previously (36). The rabbit anti-VDAC blocking antibodies were used. This antibody was reported to inhibit Bax-mediated cytochrome *c* release and membrane potential loss, without inhibiting mitochondrial respiration of cells (36). Normal rabbit IgG (NRI; Santa Cruz Biotechnology, Santa Cruz, CA) was used as a control. Either anti-VDAC antibodies (15 μg/μl) or NRI

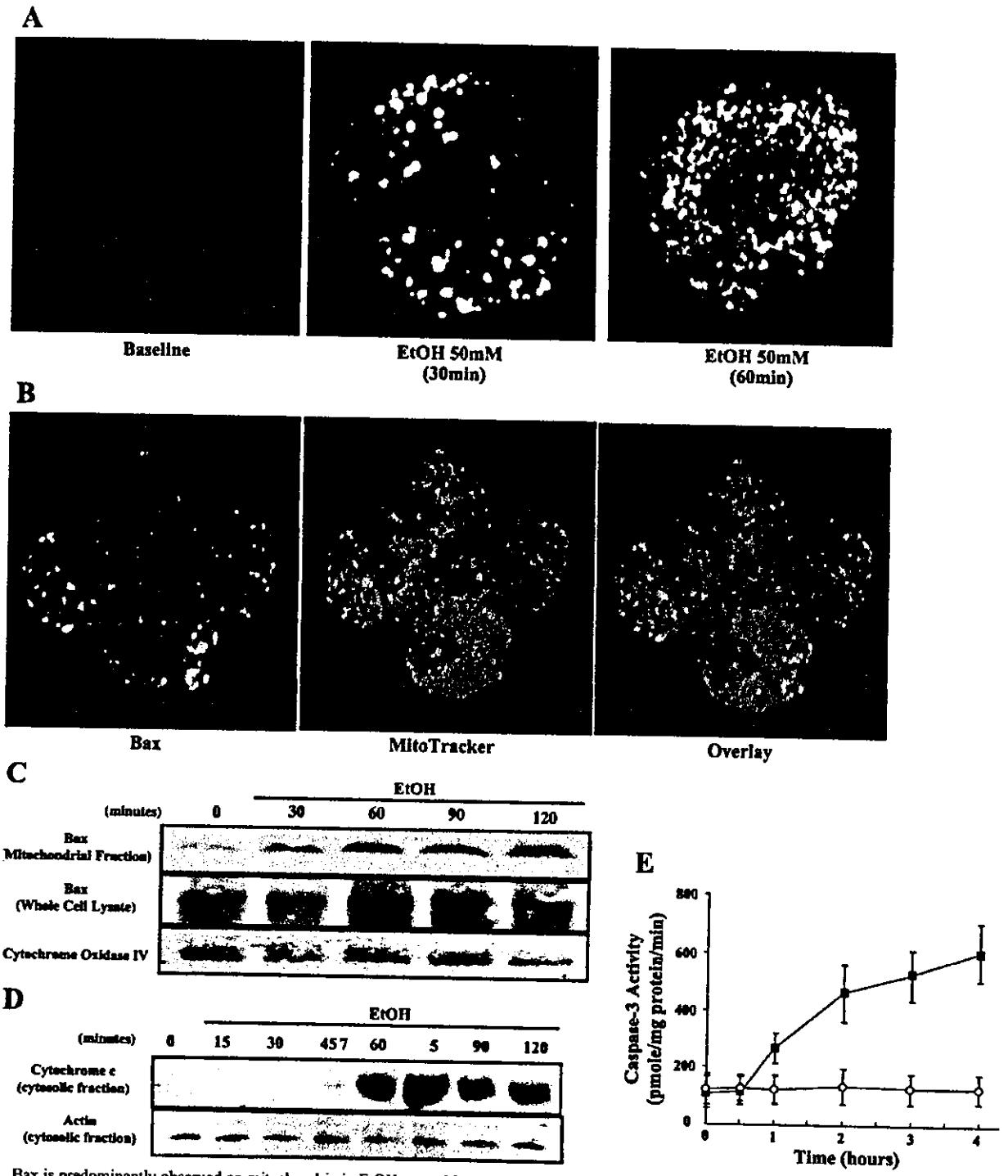

Fig. 2. Bax is predominantly observed on mitochondria in EtOH-treated hepatocytes. Hepatocytes were incubated with or without EtOH (50 mM). Immunofluorescence staining for Bax and immunoblotting for Bax and cytochrome *c* were carried out. Experiments were repeated 3 times, and the representative images were depicted. *A*: Bax immunofluorescence was visualized under a confocal microscope. Subcellular localization of Bax was altered overtime by EtOH treatment. *B*: hepatocytes were subjected to a double staining of anti-Bax and MitoTracker Red. Bax-associated fluorescence and the MitoTracker Red fluorescence are colocalized in the overlay image. *C*: mitochondrial fraction (*top*) and the whole cell lysates (*bottom*) were subjected to immunoblot analysis. Mitochondrial Bax increased within 30 min after EtOH exposure, whereas the expression level of Bax in whole cell lysates was unchanged. *D*: release of cytochrome *c* from mitochondria to the cytosol was observed by immunoblot analysis. At selected time intervals, cytosolic extracts were collected from EtOH-treated hepatocytes and exposed to an immunoblot analysis. Note that cytochrome *c* is detected in cytosolic fraction at 60 min after the exposure to EtOH. *E*: caspase-3 activity was evaluated by measuring a fluorogenic substrate Ac-Asp-Glu-Val-Asp-α-(4-methyl-coumaryl-7-amide) (DEVD-MCA) cleavage activity. Caspase-3 activity was increased at 60 min of EtOH treatment and was further elevated at the following time points.

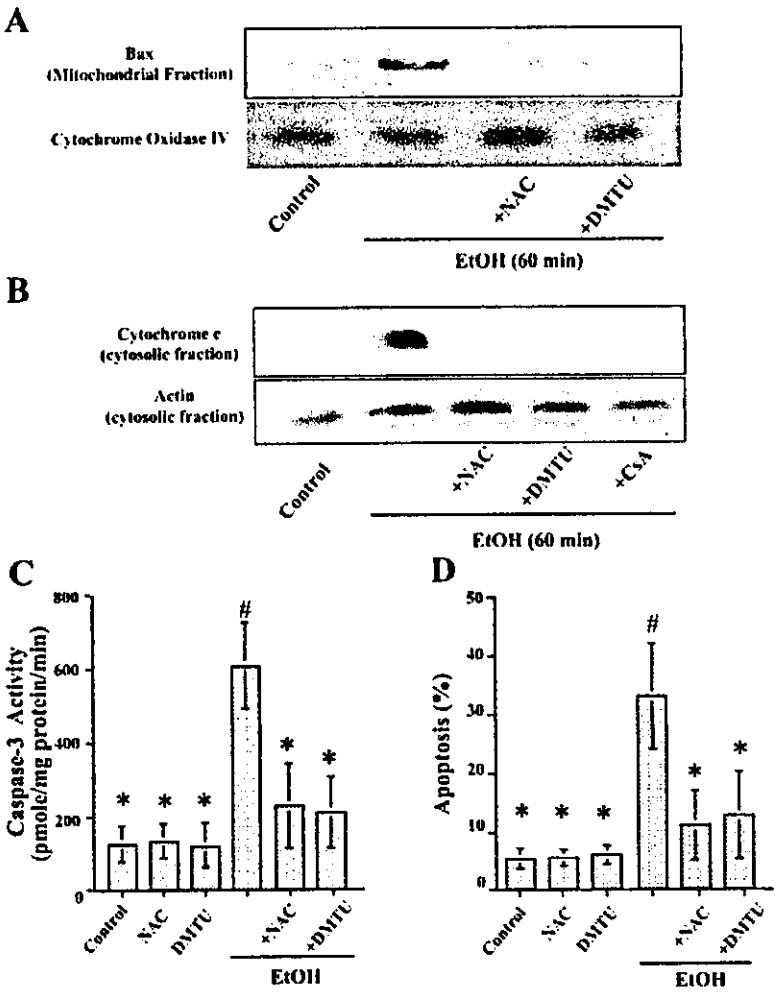

Fig. 3. Bax transmigrates to mitochondria in an oxidative stress-dependent manner. Hepatocytes were incubated with EtOH in the presence or absence of indicated inhibitors. At indicated time points, cells were harvested for mitochondria and whole cell lysate preparation. Effects of *N*-acetyl-cysteine (NAC; 5 mM), *N'*,*N'*-dimethylthiourea (DMTU; 10 mM), or cyclosporin A (CsA; 10 μM) on EtOH-induced Bax translocation to mitochondria (at 60 min) (*A*), mitochondrial cytochrome *c* release (at 60 min) (*B*), caspase-3 activation (at 2 h) (*C*), and apoptosis (at 8 h) (*D*) were evaluated. *A* and *B*: results were representative of 3 independent experiments. *C* and *D*: data were expressed as means ± SD from 5 independent experiments. #$P < 0.05$ vs. control, *$P < 0.05$ vs. EtOH by ANOVA.

was mixed with GFP (3 μg/μl) as a marker of microinjected cells and then microinjected into the cytosol of cultured hepatocytes. One hour after the injection, cells were treated with ethanol for the following 6 h.

Quantitation of apoptosis. A cell membrane-permeable nuclear binding dye Hoechst 33342 was used for evaluation of apoptosis (12). Cells were incubated with 10 μM of Hoechst 33342 for 15 min before the addition of ethanol. The blue fluorescence was visualized by using a fluorescence microscope (excitation: 330–380 nm, emission: 460 nm). Apoptosis was evaluated by morphological criteria, i.e., condensed chromatin and fragmented nuclei, and the number of cells with apoptotic nuclei was determined within a field of view at a magnification of ×400. A total of 10 randomly prechosen fields were counted per well, and the number of apoptotic cells was averaged to obtain an apoptotic index.

Caspase activity assay. Cytosolic extracts for the enzyme assay were prepared as previously described (16) with minor modifications. In brief, cells were homogenized in hypotonic buffer (in mM: 25 HEPES, 5 $MgCl_2$, 1 EGTA, 0.5 PMSF, with 2 μg/ml pepstatin and 2 μg/ml leupeptin, pH 7.5), and centrifuged for 10 min at 1,000 *g*. Caspase activity was measured by adding 50 μl of cytosol to 450 μl of assay buffer containing 25 mM HEPES (pH 7.5), 10 mM DTT, 0.1% CHAPS, 0.5 mM PMSF, 100 U/ml aprotinin, and 20 μM of fluorogenic tetrapeptide substrates Ac-Asp-Glu-Val-Asp-α-(4-methyl-coumaryl-7-amide) (DEVD-MCA; Peptide Institute, Osaka, Japan) for caspase-3 or Ac-Ile-Glu-Thr-Asp-α-(4-methyl-coumaryl-7-amide) (IETD-MCA; Peptide Institute) for caspase-8. Fluorescence (excitation: 380 nm, emission: 450 nm) was quantitated by using a fluorometer (Hamamatsu Photonics, Hamamatsu, Japan) as described previously (16).

Statistical analysis. All data represent at least three independent experiments and are expressed as the means ± SD, unless otherwise indicated. Differences between groups were compared by using ANOVA for repeated measures and a post hoc Bonferroni test to correct for multiple comparisons.

RESULTS

Ethanol causes oxidative stress predominantly within mitochondria. Because our previous study demonstrated that ethanol-induced oxidative stress targeted mitochondria (21, 22), we first evaluated subcellular localization of oxidative stress by using the oxidant-sensitive fluorescence probe DCFH-DA. DCF, an oxidized form of DCFH, fluorescence was not visible in control hepatocytes; however, the fluorescence increased significantly within 10 min after ethanol (50 mM) treatment (Fig. 1*A*). The fluorescence further increased at 20 min with an increasingly dotted pattern. To determine the exact localization of the DCF, we performed dual labeling with the mitochondria-specific dye MitoTracker Red. DCF fluorescence colocalized with MitoTracker Red fluorescence (Fig. 1*B*), suggesting that ethanol-induced oxidative stress predominantly occurs within

mitochondria. These results are consistent with our previous study showing rapid mitochondrial dysfunction after oxidative stress in ethanol-treated hepatocytes (12, 21) and emphasize the importance of oxidative stress in ethanol-induced mitochondrial injury.

Ethanol induces Bax translocation to mitochondria via an oxidative stress-dependent mechanism. Because mitochondrial dysfunction can be associated with translocation of cytosolic Bax to mitochondria (40), we then determined whether Bax transmigrates to mitochondria during ethanol-induced hepatocyte apoptosis. Bax immunofluorescence was initially diffuse, consistent with cytosolic localization. However, the Bax-associated fluorescence became dotted over time after ethanol treatment (Fig. 2*A*). To clarify the subcellular localization of Bax, mitochondria were counterstained with MitoTracker Red (Fig. 2*B*). Both Bax (green) and mitochondria (red)-associated fluorescence displayed the same pattern of fluorescence, and the overlay image showed a complete colocalization of Bax with mitochondria. Thus Bax transmigrates to mitochondria during ethanol treatment.

To confirm the transmigration of Bax to mitochondria during ethanol treatment, we performed subcellular fractionation and immunoblot analysis. Bax was initially observed in the mitochondrial fraction; however, the amount of mitochondrial Bax was significantly increased at 30 min after ethanol exposure (Fig. 2*C*), whereas total Bax expression levels within whole cell lysates were unchanged at all time points tested. Release of cytochrome *c* from mitochondria to cytosol was observed at 60 min after the addition of ethanol (Fig. 2*D*). In addition, the time point when release of cytochrome *c* starts also coincides with caspase-3 activation (Fig. 2*E*). This was consistent with our previous report (12). These results suggest that Bax translocates from cytosol to mitochondria before cytochrome *c* release and caspase-3 activation.

Previous studies (12) demonstrated that mitochondrial cytochrome *c* release is blocked by either antioxidants or the PTP inhibitor CsA. Therefore, we then tested the effects of these agents on ethanol-induced Bax transmigration. Both DMTU, a cell membrane-permeable antioxidant, and NAC, a glutathione precursor, prevented the increase in Bax association with mitochondria (Fig. 3*A*). These agents have been shown to prevent ethanol-induced elevation of DCF fluorescence (12). To confirm that the suppression of Bax translocation results in a decrease in hepatocellular apoptosis, we then evaluated the effect of antioxidants on cytochrome *c* release, caspase-3 activity, and apoptosis. Indeed, either NAC or DMTU inhibited cytochrome *c* release, caspase-3 activity, and apoptosis (Fig. 3, *B–D*), suggesting that Bax transmigration and subsequent apoptotic alteration in ethanol-treated hepatocytes is oxidative stress dependent.

Bax is not oligomerized but interacts with the mitochondrial channel protein VDAC. Bax promotes mitochondrial cytochrome *c* release by either Bax homotypic oligomerization or interaction with the PTP components such as VDAC (13, 25, 29, 40). We then examined whether Bax is oligomerized in ethanol-treated hepatocyte (1). After pretreatment with the noncleavable cross-linkers BS^3 and BSP, cells were lysed and Bax oligomerization was evaluated by Bax immunoprecipitation and immunoblot analysis (Fig. 4*A*). As a positive control for Bax oligomerization, we used protein extracts from TNF-α+ActD-treated hepatocytes. The 21-, 42-, and 63-kDa forms of

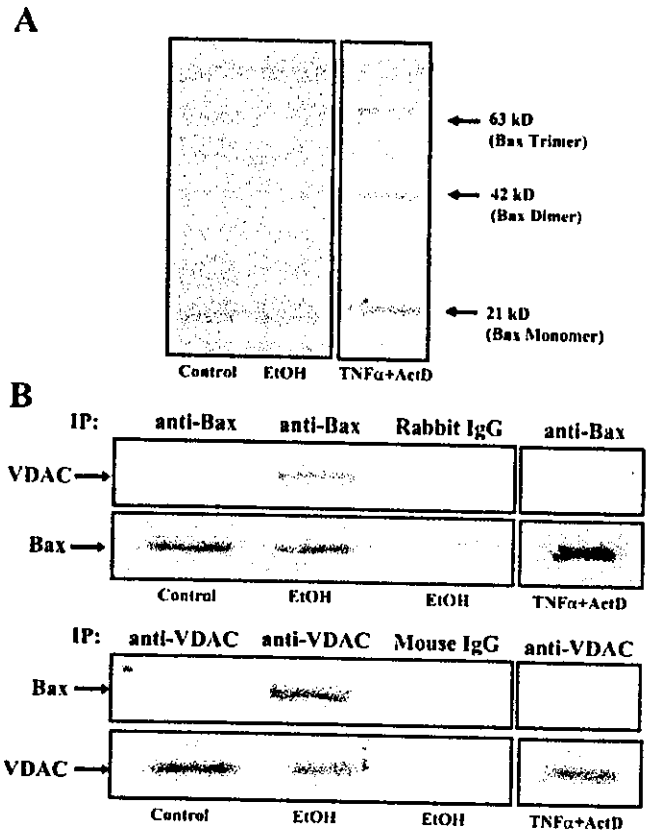

Fig. 4. Bax is not oligomerized but interacts with voltage-dependent anion channel (VDAC) in EtOH-treated hepatocytes. *A*: hepatocytes were treated with noncleavable cross-linkers bis-(sulfosuccinimidyl)suberate (BS^3) and disuccinimidyl suberate (DSS) for 30 min. Protein extracts were immunoprecipitated with rabbit anti-Bax antisera and immunoblotted with mouse anti-Bax antibody. Bax oligomerization was not observed in both control and EtOH-treated hepatocytes. Effect of TNF-α (30 ng/ml) plus actinomycin D (ActD; 0.2 μg/ml) was also evaluated. *B*: hepatocytes were treated with cleavable cross-linkers 3,3′-dithio-bis(succinimidylproprionate) (DSP) and 3,3′-dithio-bis(proprionate) (DTBP) for 30 min. Protein extracts were immunoprecipitated (IP) with either rabbit anti-Bax antisera, rabbit anti-VDAC antisera, normal rabbit IgG (NRI; as a control of anti-Bax antisera), or normal mouse IgG (as a control of anti-VDAC antisera). Immunoprecipitates were immunoblotted by indicated antibodies. Representative images were shown from 3 independent experiments. Note Bax-VDAC interactions were observed in only EtOH-treated hepatocytes.

Bax, corresponding to monomeric, dimeric, and trimeric forms of Bax, respectively, were observed in the TNF-α+ActD-treated cells. In contrast, only Bax monomers were detected in the ethanol-treated hepatocytes. In ethanol-treated hepatocytes, the density of the monomeric Bax band appears to be decreased compared with untreated controls (Fig. 4*A*). Therefore, we could not eliminate the possibility that Bax may form a larger molecular mass complex that could not be separated by the SDS-PAGE performed in the experiment.

Bax is known to form a complex with the PTP component proteins, such as VDAC, and the importance of Bax and PTP interactions in mitochondrial cytochrome *c* release has been suggested (25, 29). Therefore, we then determined whether Bax-VDAC interactions were observed in ethanol-treated hepatocytes. Hepatocytes were treated with the cleavable cross-linkers DSP and DTBP, and the cell lysates were subjected to immunoprecipitation with either anti-Bax or anti-

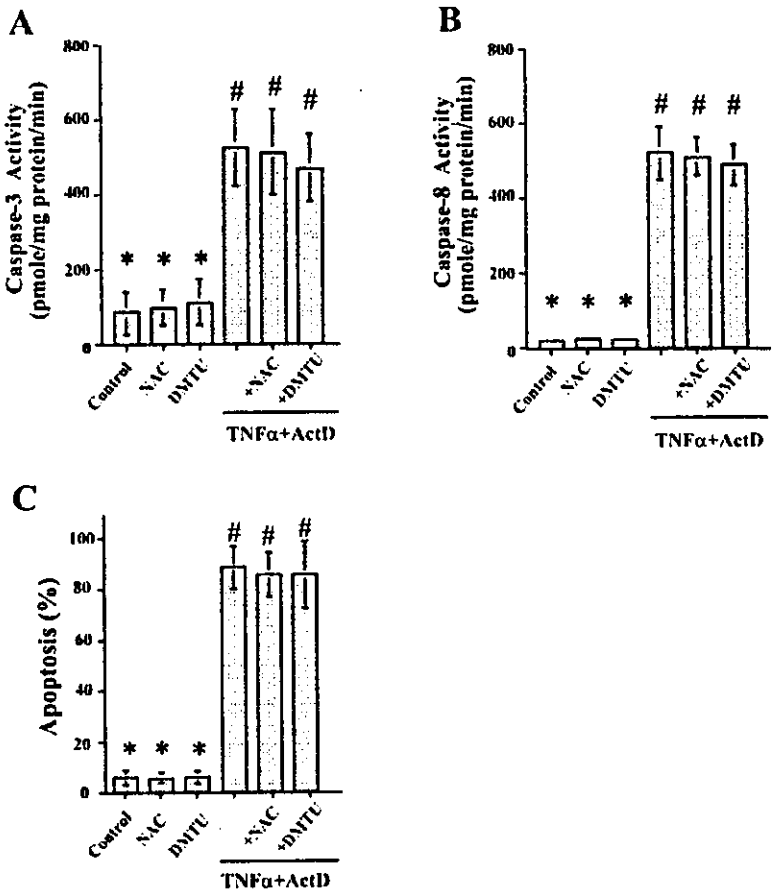

Fig. 5. TNF-α plus ActD induces caspase-8- and caspase-3-dependent apoptosis, which are not sensitive to antioxidants. Hepatocytes were incubated with or without TNF-α (30 ng/ml) plus ActD (0.2 μg/ml) in the presence or absence of indicated antioxidants. Effects of NAC (5 mM) or DMTU (10 mM) on caspase-3 (at 4 h) (*A*), caspase-8 (at 4 h) (*B*), and apoptosis (at 12 h) (*C*) were evaluated. Data were expressed as means ± SD from 5 independent experiments. #$P < 0.05$ vs. control, *$P < 0.05$ vs. TNF-α plus ActD by ANOVA.

VDAC antisera. In ethanol-treated hepatocytes, VDAC coprecipitated with Bax was observed, whereas VDAC was not observed in the precipitates from the control hepatocytes or immunoprecipitates by rabbit IgG (Fig. 4*B*). Furthermore, when the cell lysates were exposed to immunoprecipitation using an anti-VDAC antibody, Bax was only coprecipitated in ethanol-treated cells. These results suggest that Bax binds to the PTP component protein VDAC on ethanol treatment. Interestingly, the Bax-VDAC interactions were not observed in TNF-α+ActD-treated hepatocytes, suggesting that the effect of Bax on mitochondria is different between ethanol- and TNF-α+ActD-induced apoptosis.

To compare the other apoptotic machineries between these two models (ethanol vs. TNF-α+ActD), we compared other experimental manipulations in addition to an observation of BAX-VDAC interactions. TNF-α+ActD induced activation of caspase-3 and caspase-8 (Fig. 5, *A* and *B*), whereas our previous observation has shown that caspase-8 is not activated in ethanol-treated hepatocytes (12). Interestingly, antioxidants did not prevent TNF-induced caspase activation or apoptosis (Fig. 5, *A–C*).

Microinjection of anti-VDAC antibody inhibits ethanol-induced apoptosis. To determine whether the Bax-VDAC complex is essential for ethanol-induced hepatocyte apoptosis, we then microinjected anti-VDAC-blocking antibody into the cells before ethanol exposure. This antibody was raised against amino acids 151–165 of human VDAC1 where they are probably exposed to the cytoplasm, are specific for human and rat VDAC, and are able to prevent Bax-VDAC interactions (36). Anti-VDAC antibody or NRI was microinjected into the cytosol of hepatocytes, and then ethanol was added 1 h after the microinjection. Six hours after treatment with ethanol, 32.6 ± 6.9% of NRI-injected hepatocytes underwent apoptosis (Fig. 6). Microinjection of anti-VDAC antibody effectively attenuated ethanol-induced hepatocyte apoptosis, 13.6 ± 3.8% ($P < 0.05$, Fig. 6). These results suggest that VDAC-Bax associations are essential for ethanol-induced hepatocyte apoptosis.

The PTP inhibitor does not inhibit oxidative stress, Bax translocation to mitochondria, and Bax-VDAC interactions; however, these inhibitors effectively prevent cytochrome c release, caspase activation, and apoptosis. Time course observations of oxidative stress, cytochrome *c* release, and Bax translocation suggest that oxidative stress and Bax translocation to mitochondria are upstream of the mitochondrial permeability transition (MPT) and mitochondrial cytochrome *c* release within ethanol-mediated apoptotic signaling cascade. Therefore, to confirm this hypothesis, we tested whether CsA-sensitive permeability transition affects these events. CsA did not prevent the ROS generation (Fig. 7*A*), the mitochondrial translocation of Bax (Fig. 7*B*), and the formation of Bax-VDAC complex (Fig. 7*C*), whereas CsA effectively attenuated caspase-3 activation (Fig. 7*D*) and apoptosis (Fig. 7*E*). Thus oxidative stress is the first event that leads the MPT, Bax translocation to mitochondria, and Bax-VDAC interactions.

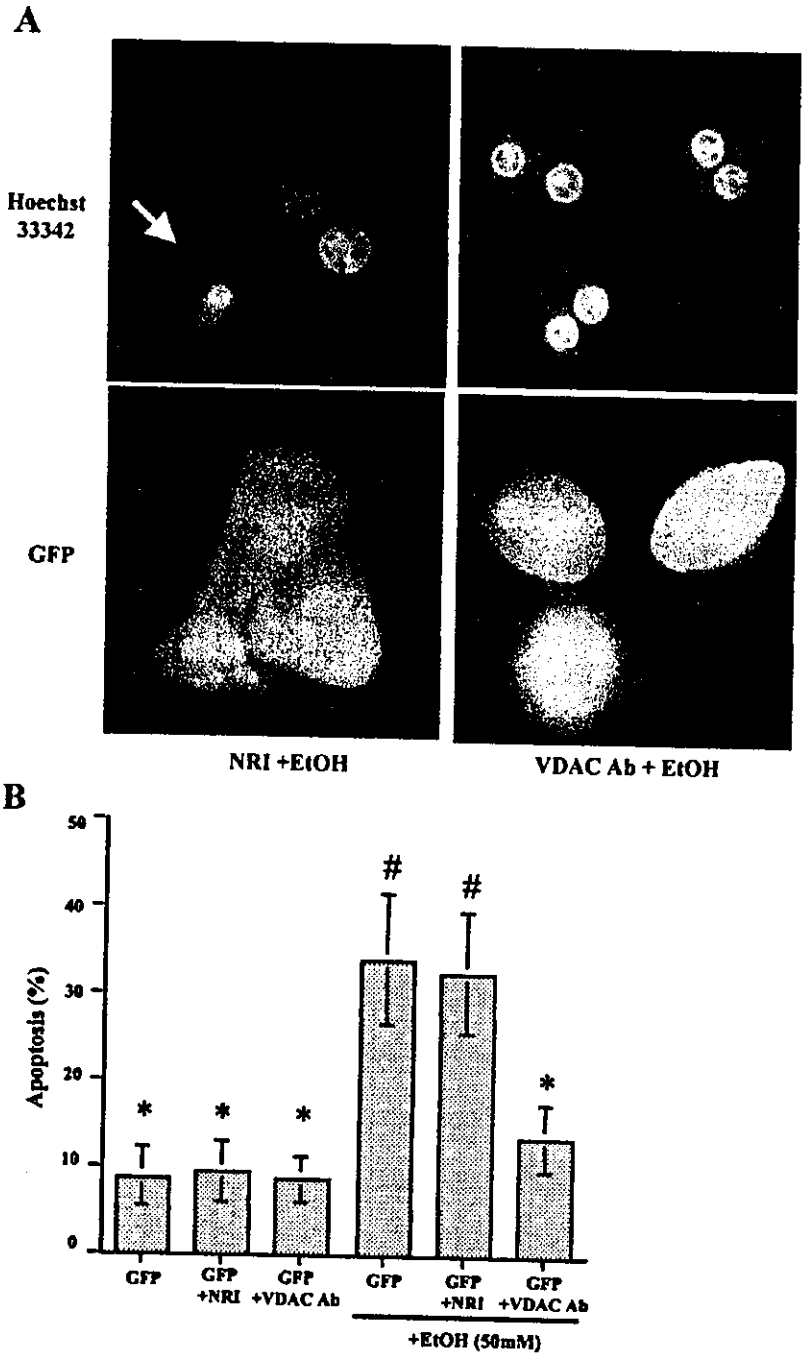

Fig. 6. Microinjection of anti-VDAC antibodies to hepatocyte inhibits EtOH-induced apoptosis. Hepatocytes were microinjected with anti-VDAC antibody or NRI at 12 μg/μl concentration. GFP (3 μg/μl) was coinjected to identify the injected cells. After incubation with EtOH (50 mM) for 8 h, cells were stained with Hoechst 33342 and observed by a fluorescent microscope. *A*: apoptosis was evaluated by morphological criteria after the Hoechst 33342 nuclear staining (blue). GFP was monitored to identify the injected cells. Representative fluorographs of control NRI-injected hepatocytes (*left*) and anti-VDAC antibody-injected hepatocytes (*right*). The arrow indicates the apoptotic cell. *B*: apoptotic nuclei were quantitated under the microscopic fields. >100 injected cells were counted for each experiment. Data were expressed as means ± SD from 5 independent experiments. #$P < 0.05$ vs. GFP + NRI-injected group, *$P < 0.05$ vs. EtOH-treated GFP + NRI-injected group by ANOVA.

DISCUSSION

The major findings of the present study relate to the cellular mechanisms of acute ethanol-induced hepatocyte apoptosis. The results indicated that *1*) acute ethanol treatment induces oxidative stress in hepatocytes within mitochondria, *2*) ethanol induces Bax translocation from the cytosol to mitochondria, *3*) Bax translocates to mitochondria before mitochondrial cytochrome *c* release, *4*) mitochondrial Bax interacts with the PTP component protein VDAC, and *5*) inhibition of Bax-VDAC interactions by anti-VDAC antibody prevents ethanol-induced apoptosis. These data implicate a role for Bax-VDAC interactions in acute ethanol-induced hepatocyte apoptosis. These observations provide further insights into mechanisms responsible for alcoholic liver injury.

Ethanol induces a hypermetabolic state in the liver that is characterized by enhanced mitochondrial respiration. The decrease in the $NAD^+/NADH$ ratio induced by acute ethanol administration may favor mitochondrial superoxide generation by increasing the electron flow along the respiratory electron transport chain (11, 15, 21). The enhanced superoxide generation increases mitochondrial lipid peroxide generation (26). Our data support these concepts by directly demonstrating

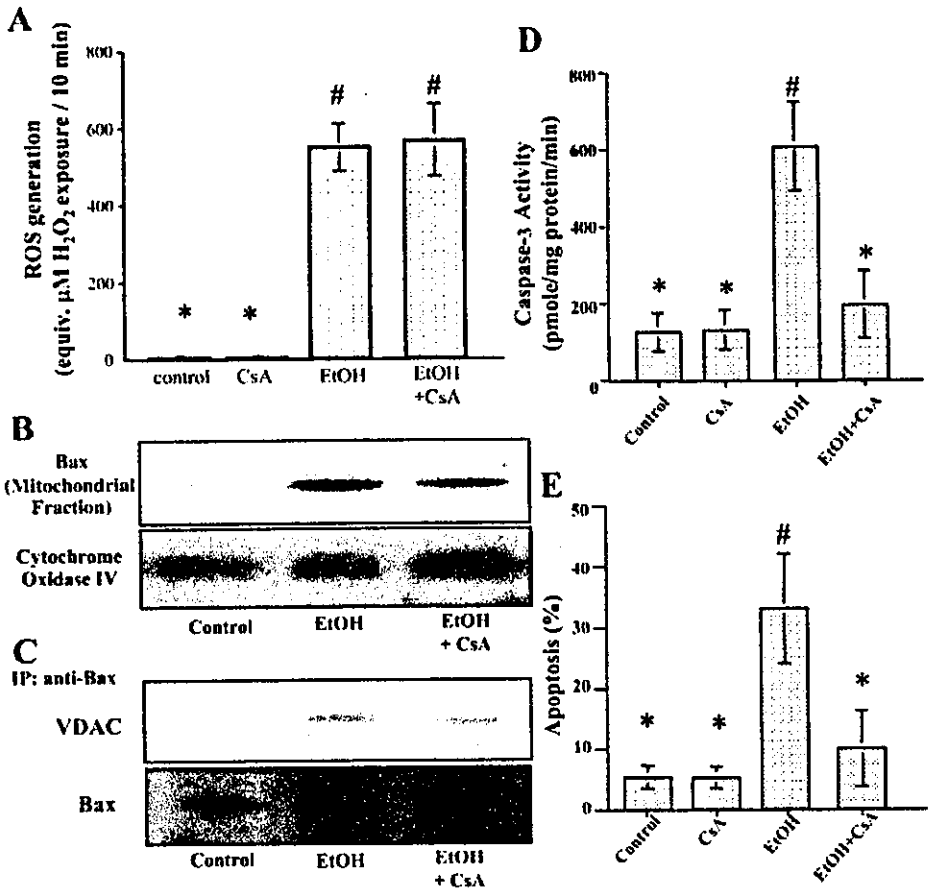

Fig. 7. Oxidative stress, Bax translocation to mitochondria, and Bax-VDAC interaction are upstream events of apoptotic mitochondrial permeability transition. Hepatocytes were incubated with or without 50 mM of EtOH in the presence or absence of CsA (10 μM). Effects of CsA on reactive oxygen species (ROS) generation determined by DCF fluorescence (*A*), Bax translocation to mitochondria (*B*), Bax-VDAC interaction (*C*), caspase-3 activity (*D*), and apoptosis (*E*) were evaluated. CsA failed to prevent oxidative-stress-associated DCF fluorescence, Bax translocation, and Bax-VDAC interaction. *A*, *D*, and *E*: data were expressed as means ± SD from 5 independent experiments. #$P < 0.05$ vs. control, *$P < 0.05$ vs. EtOH by ANOVA. *B* and *C*: results were representative of 3 independent experiments.

mitochondrial oxidative stress as visualized by an oxidant-sensitive fluorescent probe DCFH-DA during acute ethanol intoxication. Because mitochondria are the major source of ethanol-associated oxidant production, they are therefore also likely to be the first target in oxidative stress-associated injury.

In the present study, Bax was observed to translocate from the cytoplasm to mitochondria before mitochondrial cytochrome *c* release during exposure to ethanol. This observation suggests that Bax may play an important role in mitochondrial cytochrome *c* release. Bax-mediated mitochondrial cytochrome *c* release has been implicated in both death receptor-mediated and nondeath receptor pathway of apoptosis (27, 37). However, our data suggest that Bax association with mitochondria in ethanol-treated hepatocytes is distinct from the TNF-mediated death receptor signaling pathway. In the ethanol-treated hepatocytes, Bax forms a complex with the PTP component protein VDAC. In contrast, this heterotypic interaction of Bax and VDAC was not observed in TNF-α-treated cells. In death receptor-mediated pathway, Bax may form a homotypic oligomer channel on the death receptor-mediated tBid signaling (7, 20). The Bax homooligomerization may result in a formation of various oligomers of Bax complexes including dimers and trimers (1, 7). Consistent with the previous reports, we observed monomeric, dimeric, and trimeric forms of Bax in the TNF-α-treated hepatocytes. In ethanol-treated hepatocytes, Bax homotypic oligomerization was not observed. Thus ethanol may predominantly induce Bax-VDAC heterotypic interactions, whereas TNF-α may induce Bax homooligomerization.

The differences in Bax molecular complex formation may account for differences in apoptotic signals between two models (ethanol vs. TNF-α). The most significant difference is caspase-8 dependency. In the case of TNF-α, it is well accepted that death receptors such as TNF-receptor 1 can activate caspase-8. Activated caspase-8 cleaves and activates Bid. Bid and Bax (or Bak) cooperate to induce mitochondrial cytochrome *c* release on mitochondrial outer membrane. In contrast, our previous study (12) has shown that ethanol-mediated apoptosis is not mediated by caspase-8 and Bid. In the present study, we report some additional findings regarding the difference of apoptosis signaling between these two models: *1*) antioxidants effectively inhibited Bax translocation and subsequent apoptotic signals in ethanol model, whereas antioxidants failed to inhibit TNF-induced apoptosis; and *2*) ethanol induces Bax-VDAC interaction, whereas TNF does not induce detectable interaction of these two molecules. Interestingly, it has been reported that inhibitors of MPT reduced oxidative stress, whereas antioxidants reduced mitochondrial permeability in a certain caspase-8-mediated apoptosis such as bile acid (41). It would be possible that oxidative stress is more important to signal (or initiate) apoptosis in a caspase-8-independent apoptosis model.

Our previous study (12) demonstrated that acute ethanol induced an increase in the mitochondrial membrane permeabil-

ity leading to massive cytochrome *c* release. The increase in the mitochondrial permeability was evaluated by mitochondrial calcein release assay (an indicator of the permeability of both inner and outer membranes) and was likely mediated by the PTP opening because it was prevented by the PTP inhibitor CsA. In the present study, we further evaluated whether the mitochondrial Bax transmigration and the Bax-VDAC interactions are sensitive to PTP inhibitor. CsA failed to attenuate ethanol-induced mitochondrial translocation of Bax or its interaction with VDAC, suggesting that Bax-VDAC interactions observed in the ethanol-treated hepatocytes is an upstream signal of PTP opening. Because VDAC is a major component of the PTP, it would be possible that Bax-VDAC interactions may alter the PTP status, which allows cytochrome *c* to leave mitochondria. Indeed, CsA effectively prevented ethanol-induced mitochondrial cytochrome *c* release, caspase-3 activation, and apoptosis (12).

In conclusion, the present study provides an additional mechanism for acute ethanol-induced hepatocyte apoptosis. Ethanol-associated oxidative stress induces Bax transmigration to the mitochondria. Bax interacts with the PTP component protein VDAC and likely causes PTP opening, cytochrome *c* release, caspase activation, and apoptosis. Prevention of the Bax-VDAC interactions by specific anti-VDAC antibody prevented the hepatocyte apoptosis. Therefore, Bax-VDAC interaction would be a potential target for prevention of alcohol-related liver injury.

ACKNOWLEDGMENTS

The authors thank Dr. Shigeomi Shimizu (Osaka University, Osaka, Japan) for anti-VDAC antisera. We thank Dr. Gregory J. Gores (Mayo Clinic, Rochester, MN) for exciting discussion about experimental design and for manuscript preparation.

GRANTS

This study was supported by a Grant-in-Aid for Scientific Research from the Ministry of Education, Science and Culture of Japan.

REFERENCES

1. **Antonsson B, Montessuit S, Sanchez B, and Martinou JC.** Bax is present as a high molecular weight oligomer/complex in the mitochondrial membrane of apoptotic cells. *J Biol Chem* 276: 11615–11623, 2001.
2. **Benedetti A, Brunelli E, Risicato R, Cilluffo T, Jezequel AM, and Orlandi F.** Subcellular changes and apoptosis induced by ethanol in rat liver. *J Hepatol* 6: 137–143, 1988.
3. **Bernardi P.** The permeability transition pore. Control points of a cyclosporin A-sensitive mitochondrial channel involved in cell death. *Biochim Biophys Acta* 1275: 5–9, 1996.
4. **Beutner G, Ruck A, Riede B, and Brdiczka D.** Complexes between porin, hexokinase, mitochondrial creatine kinase and adenylate translocator display properties of the permeability transition pore. Implication for regulation of permeability transition by the kinases. *Biochim Biophys Acta* 1368: 7–18, 1998.
5. **Cathcart R, Schwiers E, and Ames BN.** Detection of picomole levels of hydroperoxides using a fluorescent dichlorofluorescein assay. *Anal Biochem* 134: 111–116, 1983.
6. **Drochmans P, Wanson JC, and Mosselmans R.** Isolation and subfractionation on ficoll gradients of adult rat hepatocytes. Size, morphology, and biochemical characteristics of cell fractions. *J Cell Biol* 66: 1–22, 1975.
7. **Eskes R, Desagher S, Antonsson B, and Martinou JC.** Bid induces the oligomerization and insertion of Bax into the outer mitochondrial membrane. *Mol Cell Biol* 20: 929–935, 2000.
8. **Finucane DM, Bossy-Wetzel E, Waterhouse NJ, Cotter TG, and Green DR.** Bax-induced caspase activation and apoptosis via cytochrome *c* release from mitochondria is inhibitable by Bcl-xL. *J Biol Chem* 274: 2225–2233, 1999.
9. **Goldin RD, Hunt NC, Clark J, and Wickramasinghe SN.** Apoptotic bodies in a murine model of alcoholic liver disease: reversibility of ethanol-induced changes. *J Pathol* 171: 73–76, 1993.
10. **Green DR and Reed JC.** Mitochondria and apoptosis. *Science* 281: 1309–1312, 1998.
11. **Handler JA and Thurman RG.** Redox interactions between catalase and alcohol dehydrogenase pathways of ethanol metabolism in the perfused rat liver. *J Biol Chem* 265: 1510–1515, 1990.
12. **Higuchi H, Adachi M, Miura S, Gores GJ, and Ishii H.** The mitochondrial permeability transition contributes to acute ethanol-induced apoptosis in rat hepatocytes. *Hepatology* 34: 320–328, 2001.
13. **Hsu YT, Wolter KG, and Youle RJ.** Cytosol-to-membrane redistribution of Bax and Bcl-X(L) during apoptosis. *Proc Natl Acad Sci USA* 94: 3668–3672, 1997.
14. **Huser J, Rechenmacher CE, and Blatter LA.** Imaging the permeability pore transition in single mitochondria. *Biophys J* 74: 2129–2137, 1998.
15. **Ishii H, Kurose I, and Kato S.** Pathogenesis of alcoholic liver disease with particular emphasis on oxidative stress. *J Gastroenterol Hepatol* 12: S272–S282, 1997.
16. **Jones B, Roberts PJ, Faubion WA, Kominami E, and Gores GJ.** Cystatin A expression reduces bile salt-induced apoptosis in a rat hepatoma cell line. *Am J Physiol Gastrointest Liver Physiol* 275: G723–G730, 1998.
17. **Jurgensmeier JM, Xie Z, Deveraux Q, Ellerby L, Bredesen D, and Reed JC.** Bax directly induces release of cytochrome *c* from isolated mitochondria. *Proc Natl Acad Sci USA* 95: 4997–5002, 1998.
18. **Kaplowitz N and Tsukamoto H.** Oxidative stress and liver disease. *Prog Liver Dis* 14: 131–159, 1996.
19. **Kawahara H, Matsuda Y, and Takase S.** Is apoptosis involved in alcoholic hepatitis? *Alcohol Alcohol* 29, *Suppl* 1: 113–118, 1994.
20. **Korsmeyer SJ, Wei MC, Saito M, Weiler S, Oh KJ, and Schlesinger PH.** Pro-apoptotic cascade activates BID, which oligomerizes BAK or BAX into pores that result in the release of cytochrome *c*. *Cell Death Differ* 7: 1166–1173, 2000.
21. **Kurose I, Higuchi H, Kato S, Miura S, Watanabe N, Kamegaya Y, Tomita K, Takaishi M, Horie Y, Fukuda M, Mizukami K, and Ishii H.** Oxidative stress on mitochondria and cell membrane of cultured rat hepatocytes and perfused liver exposed to ethanol. *Gastroenterology* 112: 1331–1343, 1997.
22. **Kurose I, Higuchi H, Miura S, Saito H, Watanabe N, Hokari R, Hirokawa M, Takaishi M, Zeki S, Nakamura T, Ebinuma H, Kato S, and Ishii H.** Oxidative stress-mediated apoptosis of hepatocytes exposed to acute ethanol intoxication. *Hepatology* 25: 368–378, 1997.
23. **Kurose I, Miura S, Fukumura D, Yonei Y, Saito H, Tada S, Suematsu M, and Tsuchiya M.** Nitric oxide mediates Kupffer cell-induced reduction of mitochondrial energization in hepatoma cells: a comparison with oxidative burst. *Cancer Res* 53: 2676–2682, 1993.
24. **Lemasters JJ, Nieminen AL, Qian T, Trost LC, Elmore SP, Nishimura Y, Crowe RA, Cascio WE, Bradham CA, Brenner DA, and Herman B.** The mitochondrial permeability transition in cell death: a common mechanism in necrosis, apoptosis and autophagy. *Biochim Biophys Acta* 1366: 177–196, 1998.
25. **Marzo I, Brenner C, Zamzami N, Jurgensmeier JM, Susin SA, Vieira HL, Prevost MC, Xie Z, Matsuyama S, Reed JC, and Kroemer G.** Bax and adenine nucleotide translocator cooperate in the mitochondrial control of apoptosis. *Science* 281: 2027–2031, 1998.
26. **Masini A, Ceccarelli D, Gallesi D, Giovannini F, and Trenti T.** Lipid hydroperoxide induced mitochondrial dysfunction following acute ethanol intoxication in rats. The critical role for mitochondrial reduced glutathione. *Biochem Pharmacol* 47: 217–224, 1994.
27. **Murphy KM, Streips UN, and Lock RB.** Bax membrane insertion during Fas(CD95)-induced apoptosis precedes cytochrome *c* release and is inhibited by Bcl-2. *Oncogene* 18: 5991–5999, 1999.
28. **Nanji AA.** Apoptosis and alcoholic liver disease. *Semin Liver Dis* 18: 187–190, 1998.
29. **Narita M, Shimizu S, Ito T, Chittenden T, Lutz RJ, Matsuda H, and Tsujimoto Y.** Bax interacts with the permeability transition pore to induce permeability transition and cytochrome *c* release in isolated mitochondria. *Proc Natl Acad Sci USA* 95: 14681–14686, 1998.
30. **Natori S, Rust C, Stadheim LM, Srinivasan A, Burgart LJ, and Gores GJ.** Hepatocyte apoptosis is a pathologic feature of human alcoholic hepatitis. *J Hepatol* 34: 248–253, 2001.
31. **Petit PX, Goubern M, Diolez P, Susin SA, Zamzami N, and Kroemer G.** Disruption of the outer mitochondrial membrane as a result of large